International
Progress Report

IPR-08-05

Äspö Hard Rock Laboratory

DECOVALEX

Validation of the ultrasonic borehole investigation in the TASQ tunnel

Ann Bäckström

Berg Bygg Konsult AB

February 2008

Svensk Kärnbränslehantering AB
Swedish Nuclear Fuel
and Waste Management Co

Box 250, SE-101 24 Stockholm
Phone +46 8 459 84 00

Äspö Hard Rock
Laboratory

Report no.
IPR-08-05
No.
F84K
Author
Ann Bäckström
Date
February 2008
Checked by
Rolf Christiansson
Date
2008-06-05
Approved
Anders Sjöland
Date
2008-06-09

Äspö Hard Rock Laboratory

DECOVALEX

Validation of the ultrasonic borehole investigation in the TASQ tunnel

Ann Bäckström

Berg Bygg Konsult AB

February 2008

Keywords: Ultrasonic/seismic borehole measurements, Rotational measurements, P-wave velocity, S-wave velocity, Fracture investigation

Abstract

In November 2006, a study of the ultrasonic velocity in a profile in the TASQ tunnel at Äspö HRL was performed. A profile of eight boreholes was drilled in section 47 in the TASQ tunnel. The study was performed with the aim to estimate the extent of the excavation damaged zone (EDZ) in the tunnel. In this investigation, locations of fractures crossing the boreholes were identified together with an investigation of the ultrasonic velocity in different directions out from selected boreholes. These "rotational measurements" were made to investigate the anisotropy of the rock mass.

This report presents the result obtained when comparing the measurement of the ultra sonic wave velocity and the mapping of fractures from the drillcores. A further analysis of the rotational measurements to estimate the usefulness of the ultrasonic method in the context of characterizing the rock mass surrounding the tunnel is also done. The results show that the ultrasonic method can detect and predict the location of open fractures crossing the borehole in crystalline rocks. The rotational velocity measurement produces results that indicate an effect of the tunnel on the P-wave and S-wave velocity to about 1 m outside the tunnel wall. Further out from the tunnel the P-wave start to rotate compared to the tunnel-axis which indicate a small deviation of the tunnel alignment to the general stress field. The effect of the stress field can be found in the S-wave velocity further away from the tunnel than for the P-wave. These results indicate that further research is required for full understanding of the effect of the stress field around tunnels on the ultrasonic wave velocity.

For further information of the measurement and the estimation of the extent of the EDZ a report from the Federal Institute for Geoscience and Natural Resources (BGR) in Hannover is available as an IPR-report published by SKB /Schuster, 2007/.

Sammanfattning

I November 2006 utfördes en undersökning av åtta borrhål borrade i en profil I TASQ tunneln dels genom seismiska mätningar och dels genom kartering av orienterade borrkärnor. Profilens låg i sektion 47, som motsvarar 47 m in i tunneln från mitten av huvudtunneln (TASA). Den seismiska undersökningen utfördes för att undersöka sprängskadezonen i tunneln. Den här rapporten presenterar resultaten av en jämförelse av seismikmätningarna och sprickkarteringen för att uppskatta möjligheten att identifiera sprickor med hjälp av seismikmätningar. Dessutom genomfördes rotationsmätningar från valda borrhål. Dessa rotationsmätningar användes för att undersöka bergmassans anisotropi.

Den här rapporten presenterar resultaten av en jämförelse mellan seismiska mätningar och sprickkartering av borrkärnor. En analys av rotationsmätningar har gjorts för att uppskatta användbarheten av denna seismiska metod för karakterisering av bergmassan runt en tunnel i kristallint berg. Resultaten visar att den här seimiska metoden kan identifiera positionen för öppna sprickor i kristallint berg. Rotationsmätningarna påvisar en effekt av tunneln på P-vågshastigheten som sträcker sig ca 1 m ut från tunneln. Denna påverkan beror på spänningsituationen runt tunneln. Längre ut från tunneln påvisar rotationen av P-vågshastigheten att tunnelriktningen inte är helt vinkelrät mot huvudspänningen. Effekten av spänningsfältet kan identifieras med S-våghastigheten med större precision än för P-vågshastigheten då man rör sig längre ut från tunneln. De här resultaten påvisar att det behövs ytterligare undersökningar för full förståelse av påverkan av spänningsfältet runt tunnlar på den här typen av seismiska mätningar.

För vidare information om seismikmätningarna och uppskattningen av sprängskadezonen se rapporten från Budensanstalt für Geowissenschaften und Rohstoffe (BGR) i Hannover /Schuster, 2007/.

Contents

1 Introduction

It is well known that ultrasonic measurements supply information of the sonic wave-velocity which can be used to quantify the elastic properties of the rock mass. Several investigations have been made where the detection of fractured rock have been proven using this method /Zimmerman and King, 1985; Carson and Young, 1993; Autio, 1997; Hirahara et al., 1999; Borm et al., 2003; Cardarelli et al., 2003; Klose et al., 2007/, although the content of the rock mass have to be identified and quantified in each case to be able to produce predictions.

This report contains quantitative results which show the usefulness of this method for a drilled and blasted tunnel with a tunnel axis having a high angle to the principal stress in the stress state at 450 m depth in the Äspö HRL.

The investigation has been performed in the TASQ tunnel where the rock mass are of crystalline rock types with wet and dry fractures.

The seismic method is preferable compared to electric methods, in this case, as the seismic signal produce indications of a change in elastic properties for both water filled fractures and dry fractures. The electric and electro-magnetic methods are sensitive to water filled fractures and additionally to disturbances from installations in the tunnel, whereas fractures without water will not give any indications. Thus, the indication of fractures is strongly depending on the electric conductivity of the content in the fracture using electric or electro-magnetic methods.

As the ultrasonic investigation has been made in boreholes and the cores from these bore holes has been mapped for fractures, a possibility now exist to quantify the results.

In the ultrasonic investigation, several measurements were made where the probe was rotated in different directions in the borehole. These rotational measurements have been made on different depth in two vertical boreholes, and a horizontal borehole in a profile of the tunnel. From these results, a preliminary comment on the usefulness to infer information of the stress situation from the ultrasonic method is made.

2 Objective and scope

The purpose of this report is to validate the ultrasonic measurements as an identifying method for fractures and inferring the stress situation around a tunnel in crystalline rock. The validation is performed by comparing the fracture mapping of the cores from the drill holes, in which the measurements were made, with the ultrasonic measurements. A rudimentary investigation is also made on the identification of the stress situation around tunnels using the ultrasonic method in rotational configuration. This method has been used in tunnels excavated in clay where it has been possible to derive the stress situation from these measurements /Schuster, pers. com., 20071112/.

The ultrasonic measurements were made with the BGR mini-sonic borehole probe with a maximum sampling frequency of 10 MHz. The core mapping was performed by Johan Berglund /Jonsson et al. 2008/, according to the method description SKB_MD_143.006. version. 1.0 which is an internal controlling document from Svensk Kärnbränslehantering AB (SKB).

This investigation is divided into two parts; one will investigate the suggested occurrence of fractures in the boreholes found by the seismic measurements and the other part will present the results from the rotational measurements with a discussion of the implications of these results. The first investigation will be presented in chapter 5 and the other one in chapter 6. The discussion will contain information from both investigations as will the conclusions.

3 Procedure

SKB supplied the project with eight boreholes drilled during the autumn of 2006 in the TASQ tunnel at the Äspö HRL. The boreholes were drilled in one cross section (horizontal, vertical up, vertical down and 45° inclined upwards with diameters of 92 mm and lengths of about 3 m (Figure 4-2). All boreholes were used for ultrasonic interval velocity measurements with a mini sonic borehole probe. Furthermore, rotational measurements at different depths were done in two vertical oriented boreholes and one horizontal borehole.

The measurements took place between the 28th and 30th of November 2006. All tasks of the measurements were performed according to the activity plan for seismic measurements in the TASQ tunnel /Bäckström, 2006/. The ultrasonic measurement techniques used as well as the interpretation of the measurements and the results used are described in the IPR-report by Schuster /2007/ and for further information about the technique the reader is referred to Schuster and Alheid /2002/.

The core mapping of the eight cores was performed by Johan Berglund. The fractures and other structures (such as: rock type boundaries, brecciated zones and dykes) identified from the ultrasonic measurements were correlated with the cores using the mapping results. The cores were supplied by the Äspö Laboratory for photography and observations involved in this investigation performed by Ann Bäckström.

4 Equipment

Within the framework of the project DECOVALEX IV, Task2 (project no: TDF 84 and activity plan: AP-TDF84-06-051, internal document for SKB) ultrasonic borehole measurements were performed by BGR in eight boreholes and additionally between two boreholes at the Äspö Hard Rock Laboratory, Sweden. These measurements aimed at the detection and characterization of the excavation disturbed / damaged zone (EdZ/EDZ) with the help of seismic borehole measurements.

All boreholes are located in one cross section in the TASQ tunnel at the 450 m level. Figure 4–1 gives an impression of the in-situ measurement conditions in the TASQ tunnel. The tunnel floor is blasted with a circular profile however, as seen in Figure 4–1 a road-bed has been installed to facilitate access. The borehole locations are shown on a true profile of the tunnel provided from a geometric laser scanning provided by Feng Quanghong at Berg Bygg Konsult AB and can be seen in Figure 4-2.

Borehole coordinates were provided by (SKB). The diameters of the boreholes were 92 mm. All the boreholes were dry or only slightly wet except for borehole KQ0047G01 (in the floor). Borehole KQ0047G01 was filled up with water and was pumped out before the measurement.

Figure 4–1. *Ultrasonic measurements with the BGR mini sonic probe in the TASQ tunnel.*

4.1 Ultra sonic measurements and configurations

All ultrasonic borehole methods applied in this investigation are discussed in detail in Schuster and Alheid /2002/. More information of this particular seismic measurement campaign can also be found in /Schuster, 2007/.

Measurements of the interval velocity are performed along single boreholes in order to quantify the change in velocity along the boreholes. The seismic velocities are measured at different interval, typically about 10 cm to 30 cm. A Budesanstalt für Geowissenschaften und Rohstoffe (BGR) mini-sonic borehole probe with one source and three receivers was used. The measurements start at the tunnel's wall. Then the probe is moved progressively down the borehole. This method then reveals the seismic velocity as a function of distance from the tunnel surface. The advantage of this method is that the length of the ray path is independent of the measuring depth. Thus the signal to noise ratio and the frequency content of the signals depend neither on the depth nor on the absorbing discontinuities outside the actual interval. Due to this, the measurements only reflect the conditions within the measuring interval.

The BGR mini-sonic borehole probe uses a piezoelectric transducer as a seismic source.

Three piezoelectric transducers at distances of 10 cm, 20 cm and 30 cm from the source are used as receivers (see Figure 4–3). The transducers were coupled to the borehole wall by pneumatic cylinders. The source signal and the three received signals are passed through a signal conditioning unit to a four channel digital storage oscilloscope (Nicolet 440) with a 12 bit dynamic range. The maximum sampling frequency is 10 MHz. In order to increase the signal to noise ratio, 200 single measurements are averaged (stacked). Figure 4-4 shows a flow chart of the data acquisition system.

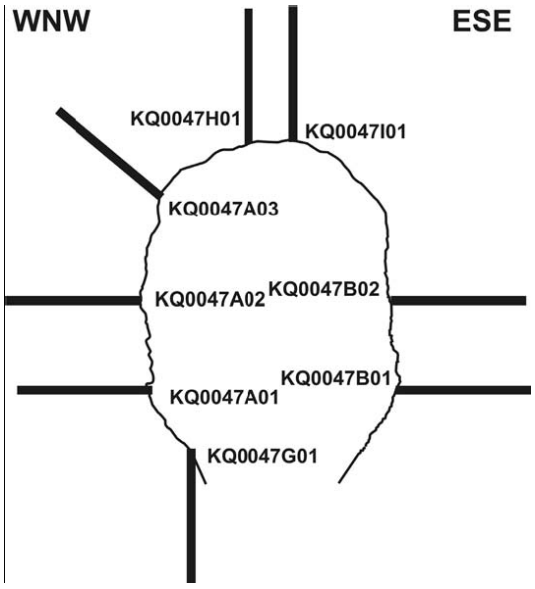

Figure 4–2. *The cross section of the TASQ tunnel and the locations of the eight boreholes used for the investigations. Diameters of the boreholes are 92 mm. View from the entrance (SSW) towards the heading face of the tunnel (NNE).*

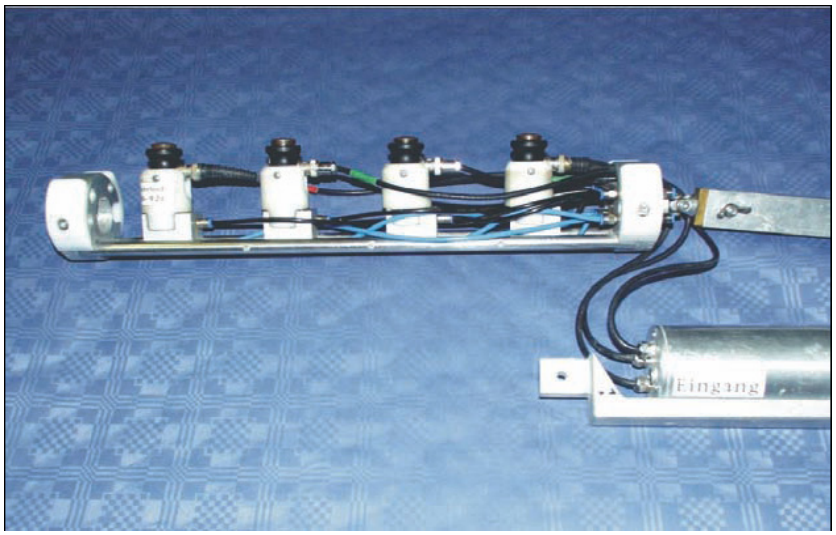

Figure 4–3. *BGR-mini-sonic borehole probe.*

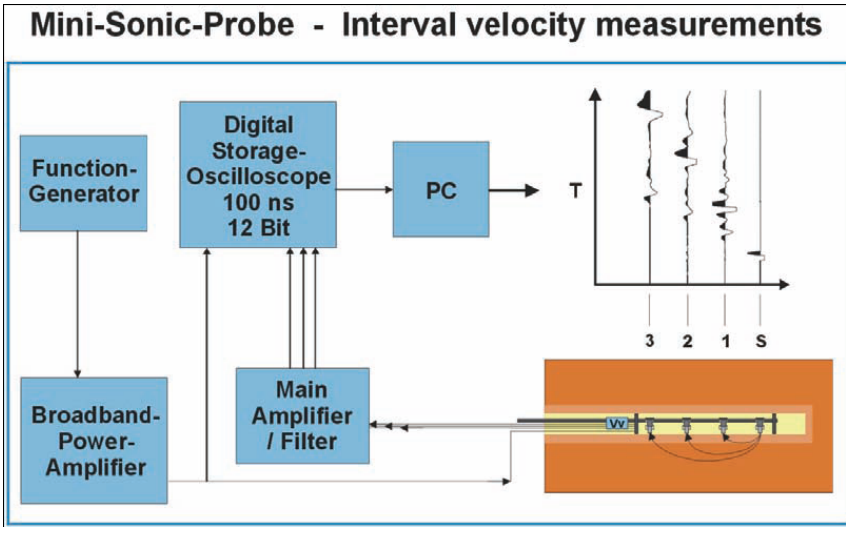

Figure 4–4. *Flow chart of seismic interval velocity measurements.*

5 The fracture investigation

The BGR team suggested several locations of large fractures crossing the boreholes. As the boreholes were mapped with respect to the fractures, the suggested fractures could be identified. The results from the seismic interval measurements in the different boreholes, from the report /Schuster, 2007/, are reproduced in Table 5-1. In the seismic measurements, the results from the interval measurements were plotted as P-wave velocity, normalized amplitude, amplitude, apparent frequency and S_V-wave velocity (Shear- wave velocity measured vertically when the P-wave velocity was measured horizontally), and its normalized amplitude, amplitude and apparent frequency. From these results, the ratio between P-wave velocity and S_V-wave velocity was calculated as well as the dynamic pseudo elastic parameters; Poisson's ratio, dynamic elastic modulus and dynamic modulus of rigidity. For the dynamic pseudo elastic parameters and more information on the derivation of these parameters see Schuster, /2007/.

Table 5-1. Possible location of cracks or fractures according to signal analyses of interval velocity data, data reprinted from /Schuster, 2007/.

Boreholes KQ0047…	Possible cracks or fractures along the borehole (cm)
A01	20-25, 70-75
A02	55-60, 70-80, 120-125
A03	(155-165)?
B01	No fractures found
B02	No fractures found
G01	(15-40)?, 40, (205-215)?
H01	(10-20)?, (170)?
I01	5-10, (85-90)?

5.1 Description of the cores

The rock type characterisation was made according to Stråhle, 2001 using the SKB mapping system (Boremap). The information has been reported by Berglund, 2007 and retrieved from the SKB database SICADA /SICADA. 2007-06-19/. All drillcores from the eight boreholes were described. With the results obtained from this description, the cores were examined in order to identify specific fractures indicated from the seismic measurements.

5.1.1 KQ0047A01

The drillcore from borehole KQ0047A01 is about 3.2 m. From the geological mapping, five open fractures has been mapped together with 13 sealed fractures /SICADA. 2007-06-19/(Figure 5-1).

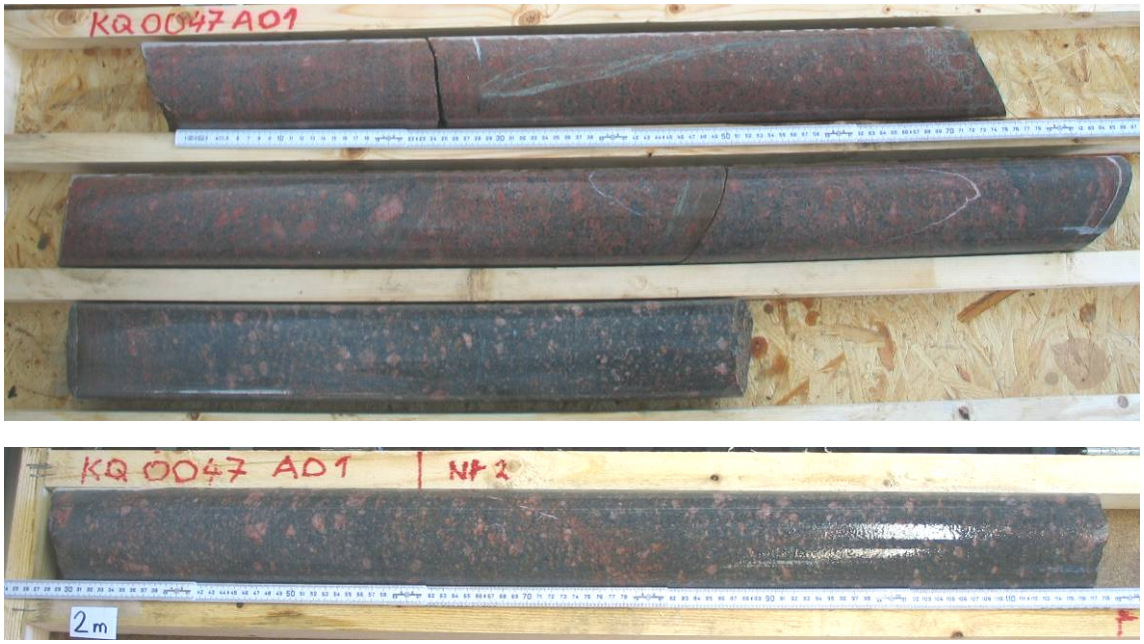

Figure 5–1. *Drillcore from the borehole KQ0047A01.*

5.1.2 KQ0047A02

The drillcore from borehole KQ0047A02 is about 3 m. From the geological mapping, 17 open fractures have been mapped together with eight sealed fractures /SICADA. 2007-06-19/ (Figure 5-2).

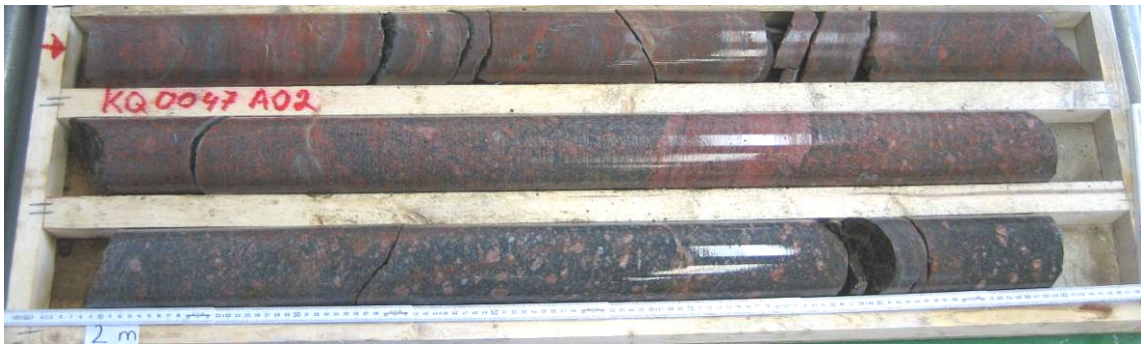

Figure 5–2. *Drillcore from the borehole KQ0047A02.*

5.1.3 KQ0047A03

The drillcore from borehole KQ0047A03 is about 3 m. From the geological mapping seven open fractures has been mapped together with four sealed fractures /SICADA. 2007-06-19/ (Figure 5-3).

Figure 5–3. *Drillcore from the borehole KQ0047A03.*

5.1.4 KQ0047B01

The drillcore from borehole KQ0047B01 is about 3 m. From the geological mapping two open fractures has been mapped together with seven sealed fractures /SICADA. 2007-06-19/ (Figure 5-4).

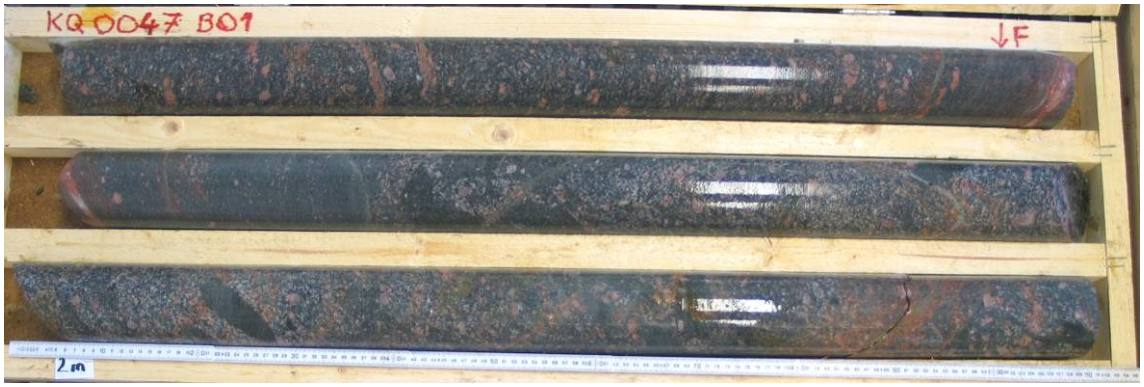

Figure 5–4. *Drillcore from the borehole KQ0047B01.*

5.1.5 KQ0047B02

The drillcore from borehole KQ0047B02 is about 3.2 m. From the geological mapping 12 open fractures has been mapped together with five sealed fractures /SICADA. 2007-06-19/ (Figure 5-5).

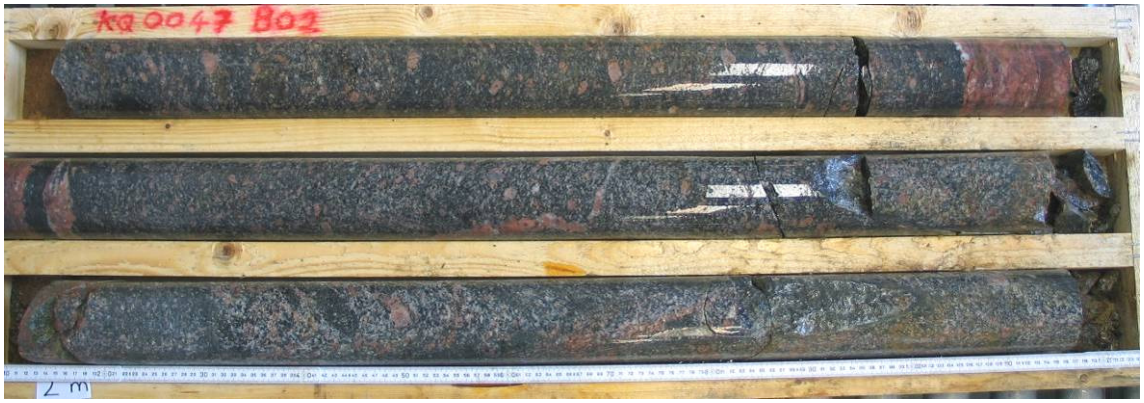

Figure 5–5. *Drillcore from the borehole KQ0047B02.*

5.1.6 KQ0047G01

The drillcore from borehole KQ0047G01 is about 3.1 m. From the geological mapping 18 open fractures has been mapped together with 12 sealed fractures /SICADA. 2007-06-19/ (Figure 5-6).

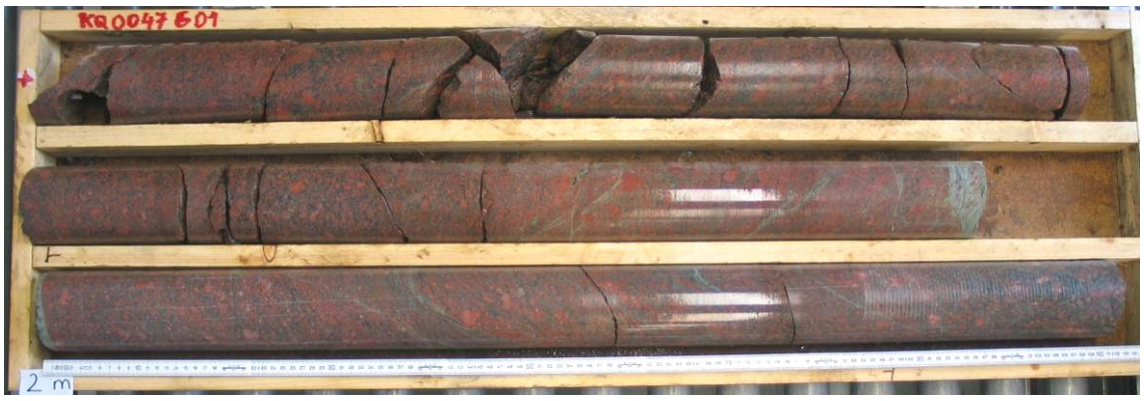

Figure 5–6. *Drillcore from the borehole KQ0047G01.*

5.1.7 KQ0047H01

The drillcore from borehole KQ0047H01 is about 3.1 m. From the geological mapping three open fractures has been mapped together with seven sealed fractures /SICADA. 2007-06-19/ (Figure 5-7).

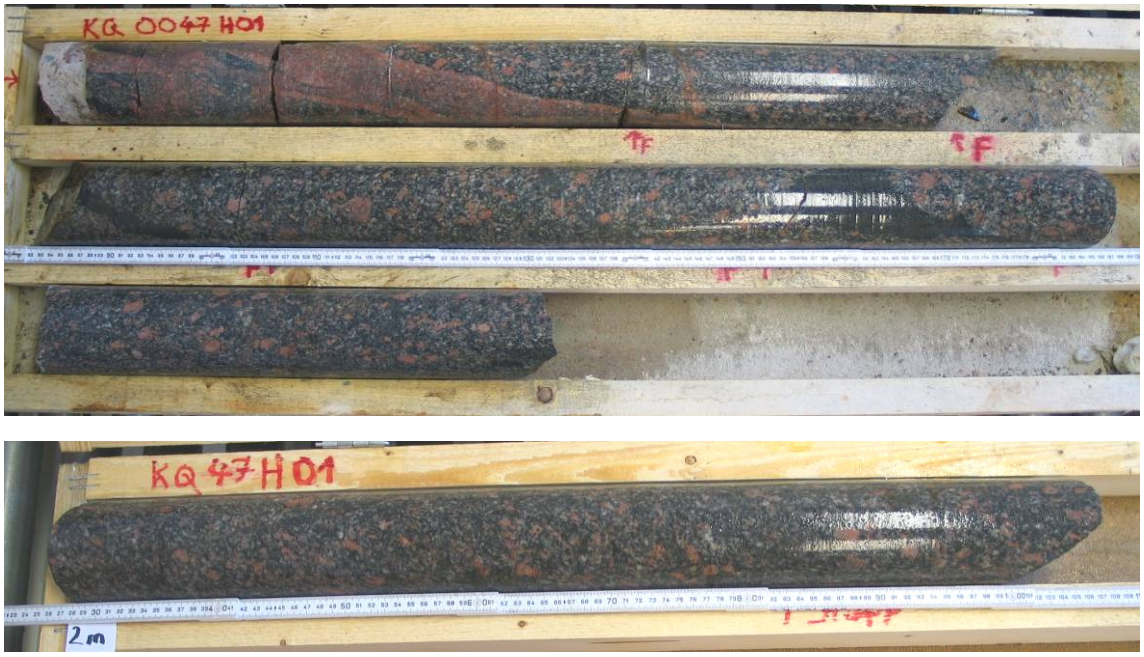

Figure 5–7. *Drillcore from the borehole KQ0047H01.*

5.1.8 KQ0047I01

The drillcore from borehole KQ0047I01 is about 3.1 m. From the geological mapping two open fractures has been mapped together with 13 sealed fractures /SICADA. 2007-06-19/ (Figure 5-8).

Figure 5–8. *Drillcore from the borehole KQ0047I01.*

5.2 Results from the core investigation

In this section, selected results from the seismic interval measurements are reproduced from the report /Schuster, 2007/ for each borehole. The information selected is: plots of the P-wave velocity along the boreholes, and plots of the properties of the P-wave. The suggested fracture sections are also derived from the seismograms which are not reproduced here.

This information is compared with the fracture mapping made on the drill cores by Berglund /Jonsson et al., 2008/. The fractures have been divided into open or sealed fractures in the drill core. The fractures are only indicated as certainly opened when they can be identified as opened in the images of the borehole wall so called BIPS images (see Appendices). If the fractures were likely to have been sealed when they were still in the rock mass i.e. they cannot be identified as opened in the BIPS image they are identified in the geological mapping as probable or possible. The precision of the seismic measurements from the BGR team is stipulated as ±0.05 m whereas the precision of the geological mapping by Berglund /Jonsson et al., 2008/ is ± 0.001 m.

5.2.1 KQ0047A01

In this borehole the fractures are indicated at depth 0.2-0.25 m and 0.7-0.75 m according to the seismic measurements (Figure 5-9).

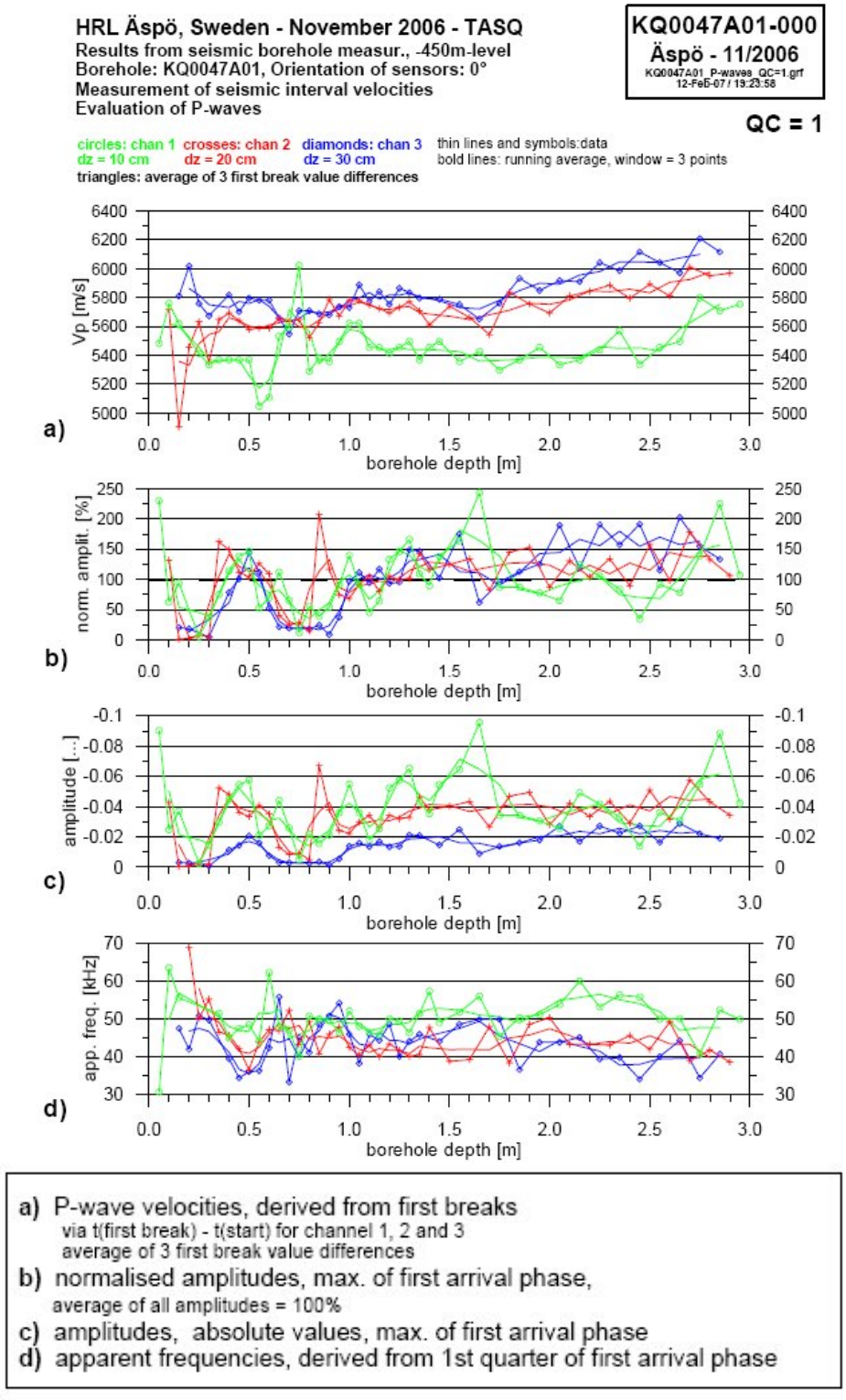

Figure 5–9. *The results from the seismic investigation of borehole KQ0047A01 /Schuster, 2007/.*

In section 0.2-0.25 m (Table 5-1), a fracture exist which is also visible in the BIPS image from the borehole wall (see also Appendix A.1.). This fracture is located 0.248 m into the borehole. As seen in Figure 4-2, this borehole is a sub-horizontal borehole into the WNW wall at a level of about 3 m above the roadbed in the tunnel. The fracture is filled with four minerals according to the core-mapping made by Berglund /Jonsson et al., 2008/. Its surface is described as irregularly rough, (see also Figure 5-10 and Figure 5-11).

The minerals coating the fracture surface are in order of decreasing amount: adularia, calcite, laumontite and prehnite. Its width (including the fracture filling minerals) is 1.5 mm and its aperture is 1 mm. This fracture can be found in the BIPS image of the borehole wall (Appendix. A.1.).

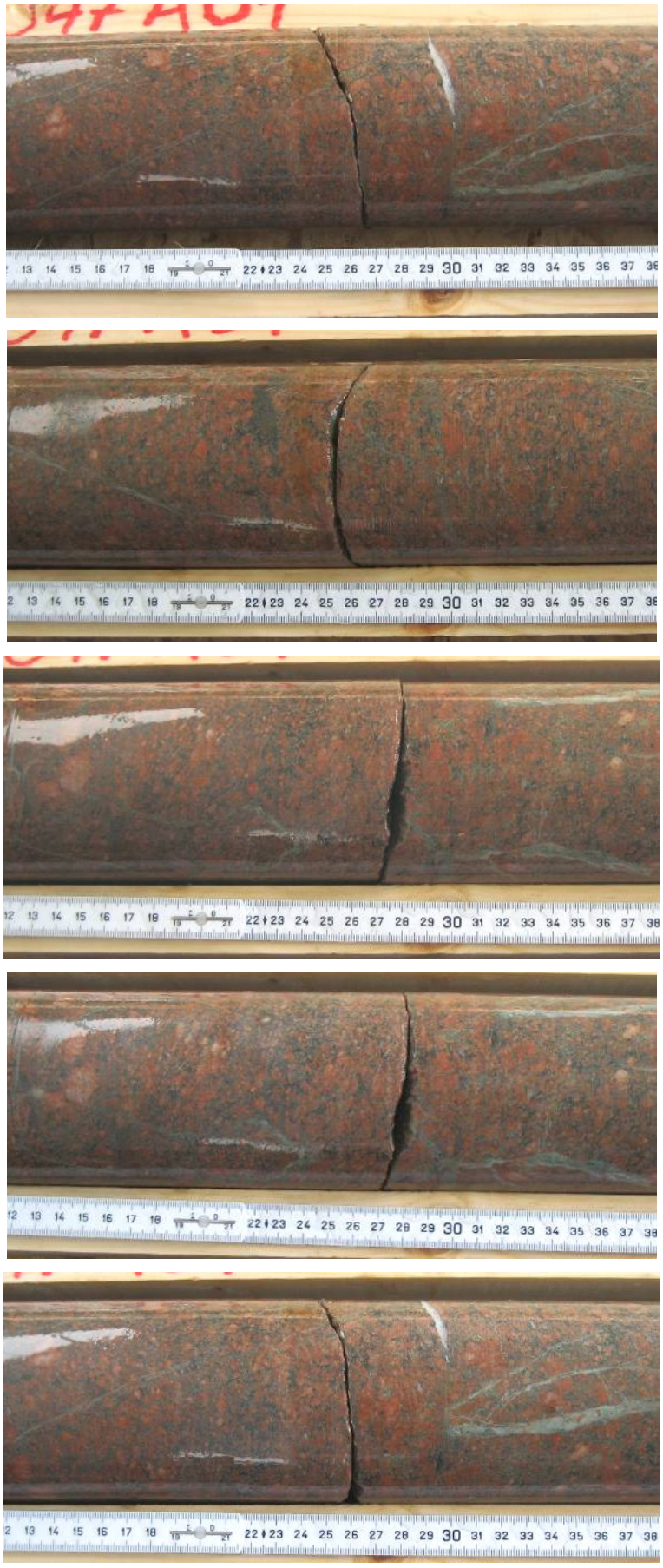

Figure 5–10. *The section including 0.2-0.25 m from the core. In different rotation.*

Figure 5–11. *The fracture surface at 0.248 m from the core in dry condition.*

The next section suggested to include a fracture is the area 0.70-0.75 m (Table 5-1). At this location, an open fracture with the fracture minerals: calcite, prehnite, chlorite and adularia is found. These fracture surfaces is planar and smooth which, together with the existence of fracture minerals, implies that this fracture is a reopened fracture (Figure 5-12 and Figure 5-13). The fracture was likely located in the rock mass when it was reopened because it can be seen as opened in the BIPS image (see appendix A.1.). It is therefore likely that this is a genuine open fracture in the rock mass surrounding the tunnel and it has been identified with the seismic measurements.

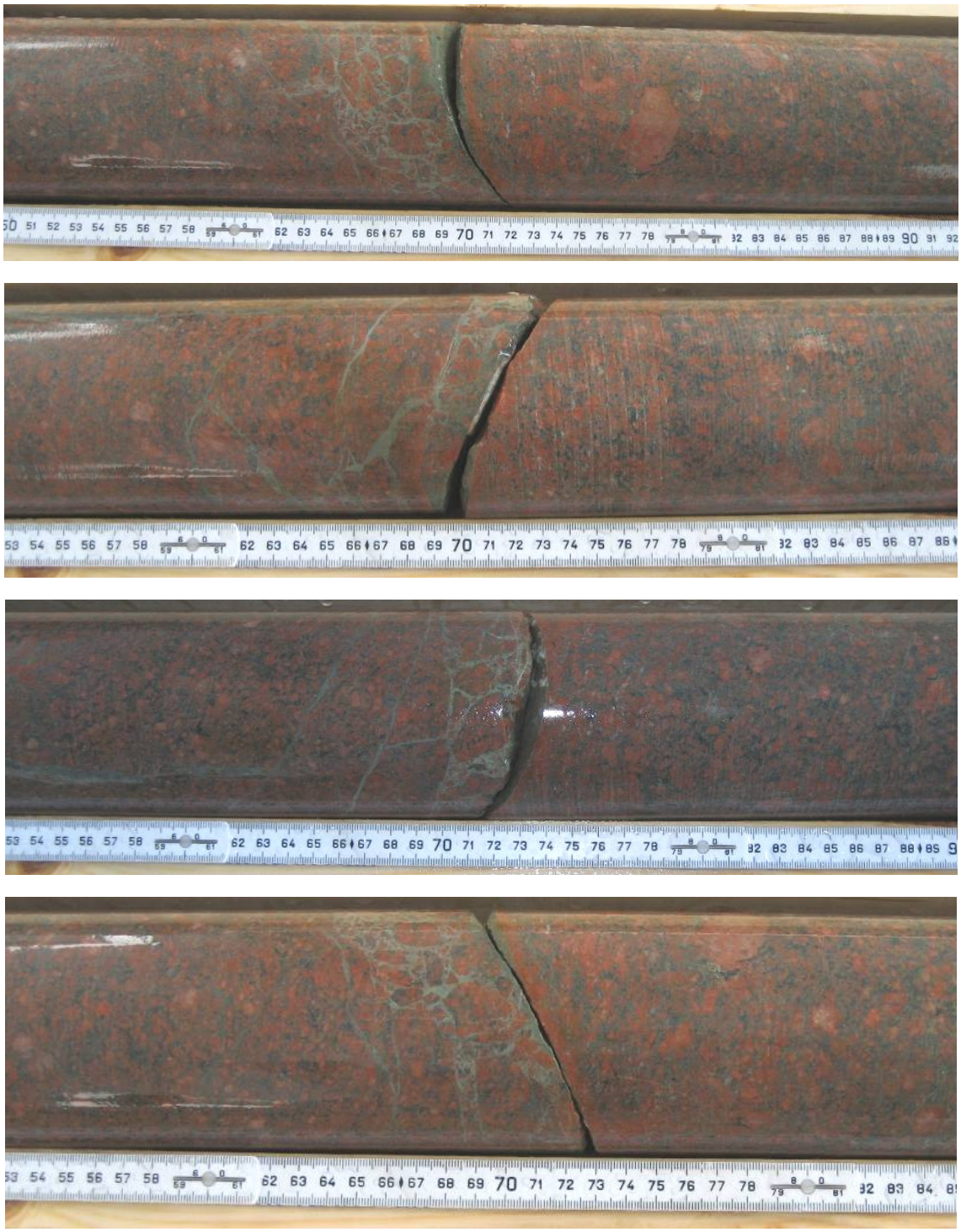

Figure 5–12. *The section including 0.7-0.75 m from the core. In different rotation.*

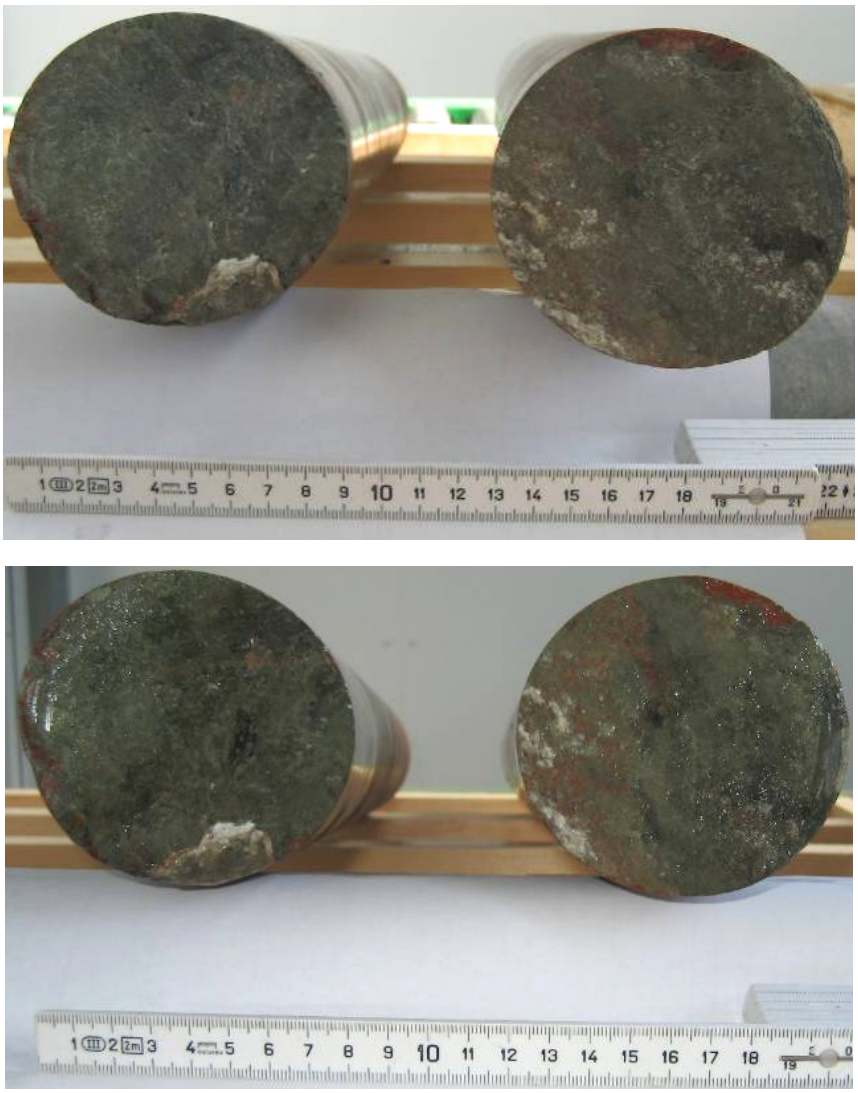

Figure 5–13. *The fracture surface for the fracture at 0.743 m in the core. Dry and wet surface.*

In this core three other fractures have been reported in the geological mapping although they were not identified in the seismic measurements. It is fractures that can have been reopened by the core handling. They are all reported as possible or probable in the geological mapping, and not certain. As an example, one of them, at depth 1.327 m has been presented in Figure 5-14. It is likely that this is a reopening of a fracture in a sealed fracture network due to core handling or drilling. This fracture is filled with chlorite and calcite as seen in Figure 5-15. The fracture surface is described as a rough surface with an irregular roughness. In the BIPS images this fracture is not opened like the two previous fractures (Appendix. A.1). The fact that the fracture can not be identified as opened in the BIPS image and that the surface is quite rough implies that this fracture have been opened by the core handling, and thus would not be seen in the seismic measurements in the borehole wall.

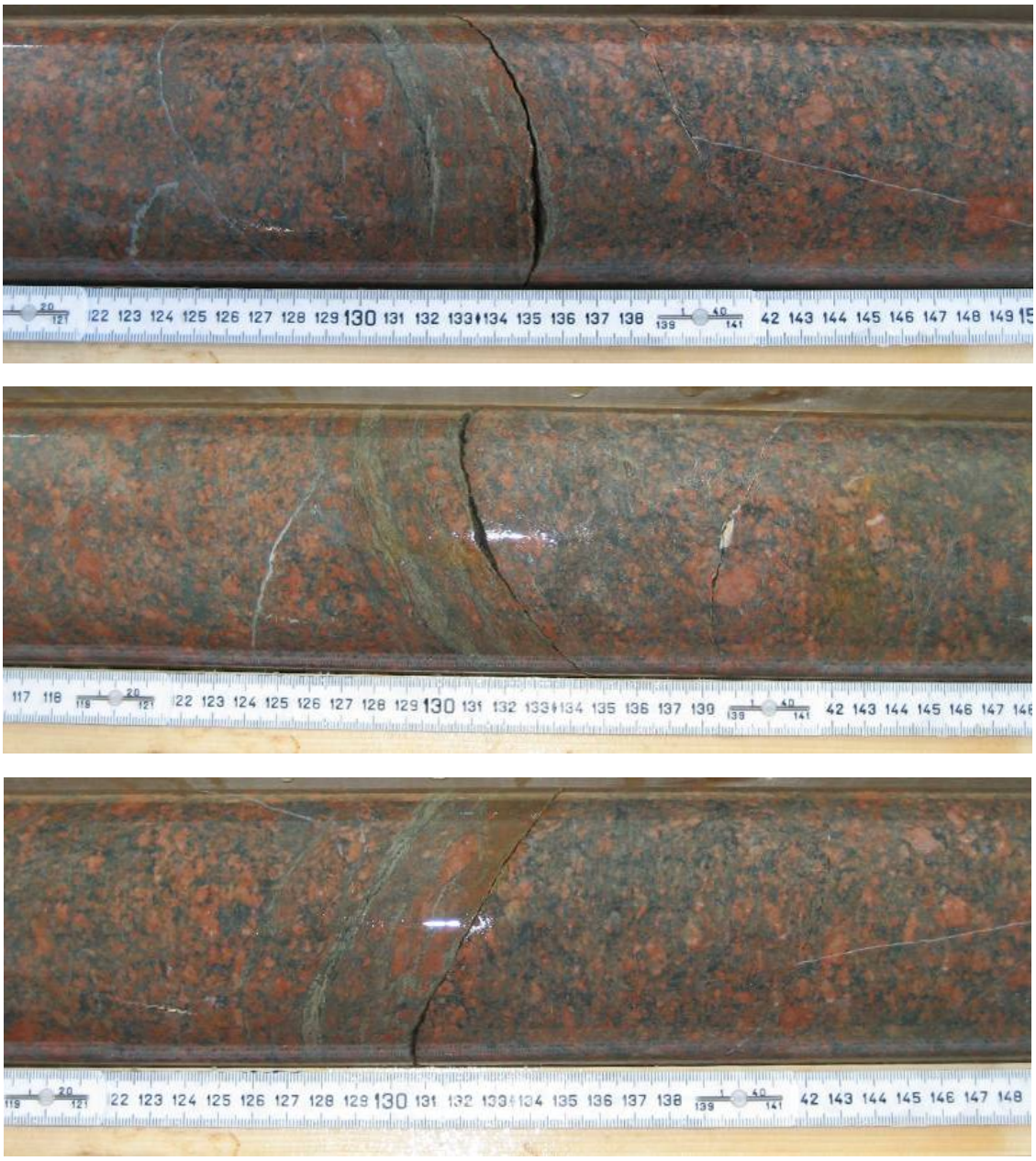

Figure 5–14. *The fracture at 1.327 m depth from the core. In different rotation.*

Figure 5–15. *The fracture surface for the fracture at 1.327 m in the core. Dry and wet surface.*

5.2.2 KQ0047A02

In this borehole, the fractures are indicated at depth 0.55-0.6 m, 0.70-0.8 m and 1.20-1.25 m according to the seismic measurements (Figure 5-16). When investigating the section between 0.55-0.6 m, a fracture can be found in the drillcore. The fracture at 0.592 m is filled with phrenite and the surface is smooth according to the geological mapping by Berglund (Figure 5-17 and Figure 5-18). A clear open fracture can be seen in the BIPS image of this borehole (see appendix A.2.).

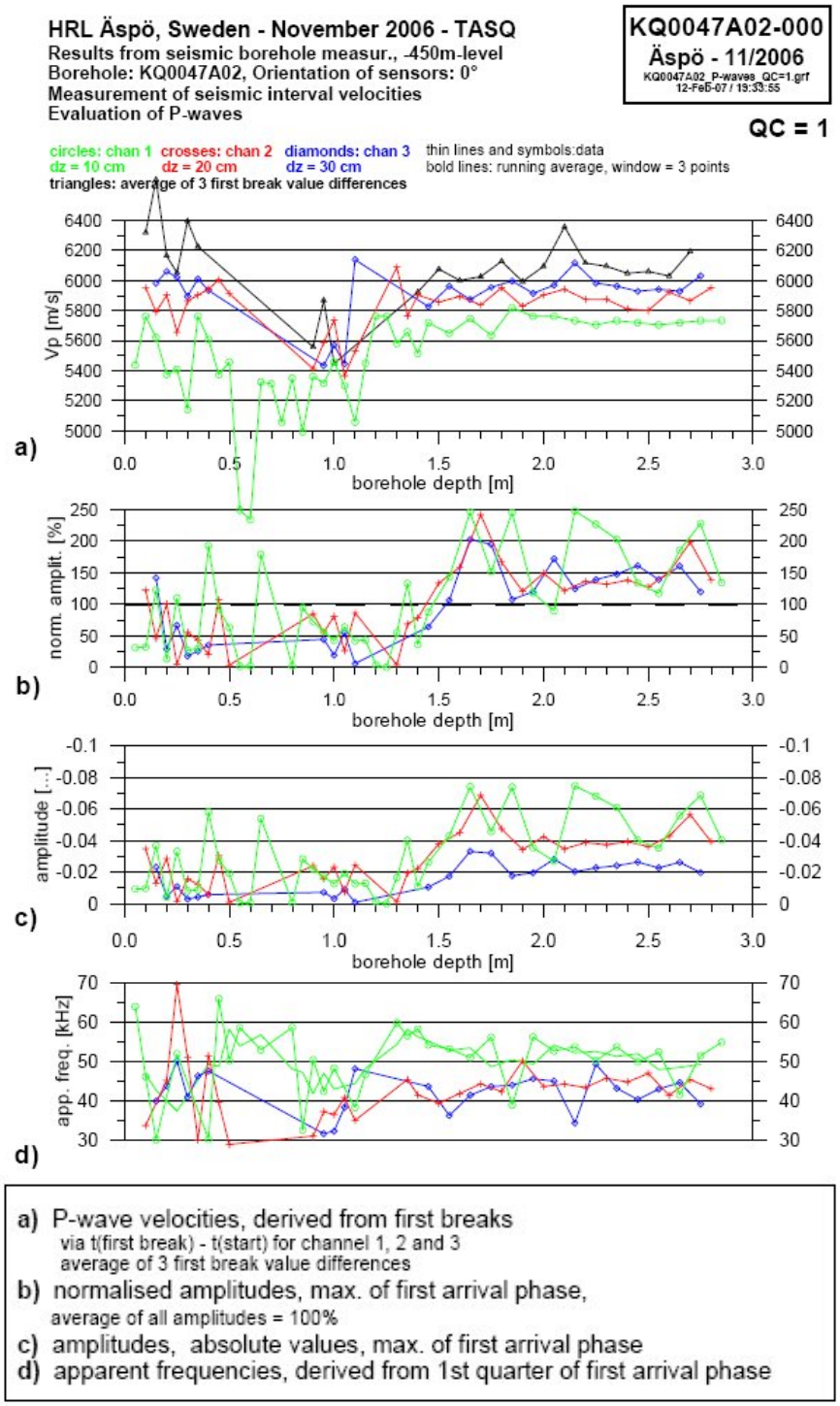

Figure 5–16. *The results from the seismic investigation of borehole KQ0047A02 /Schuster, 2007/.*

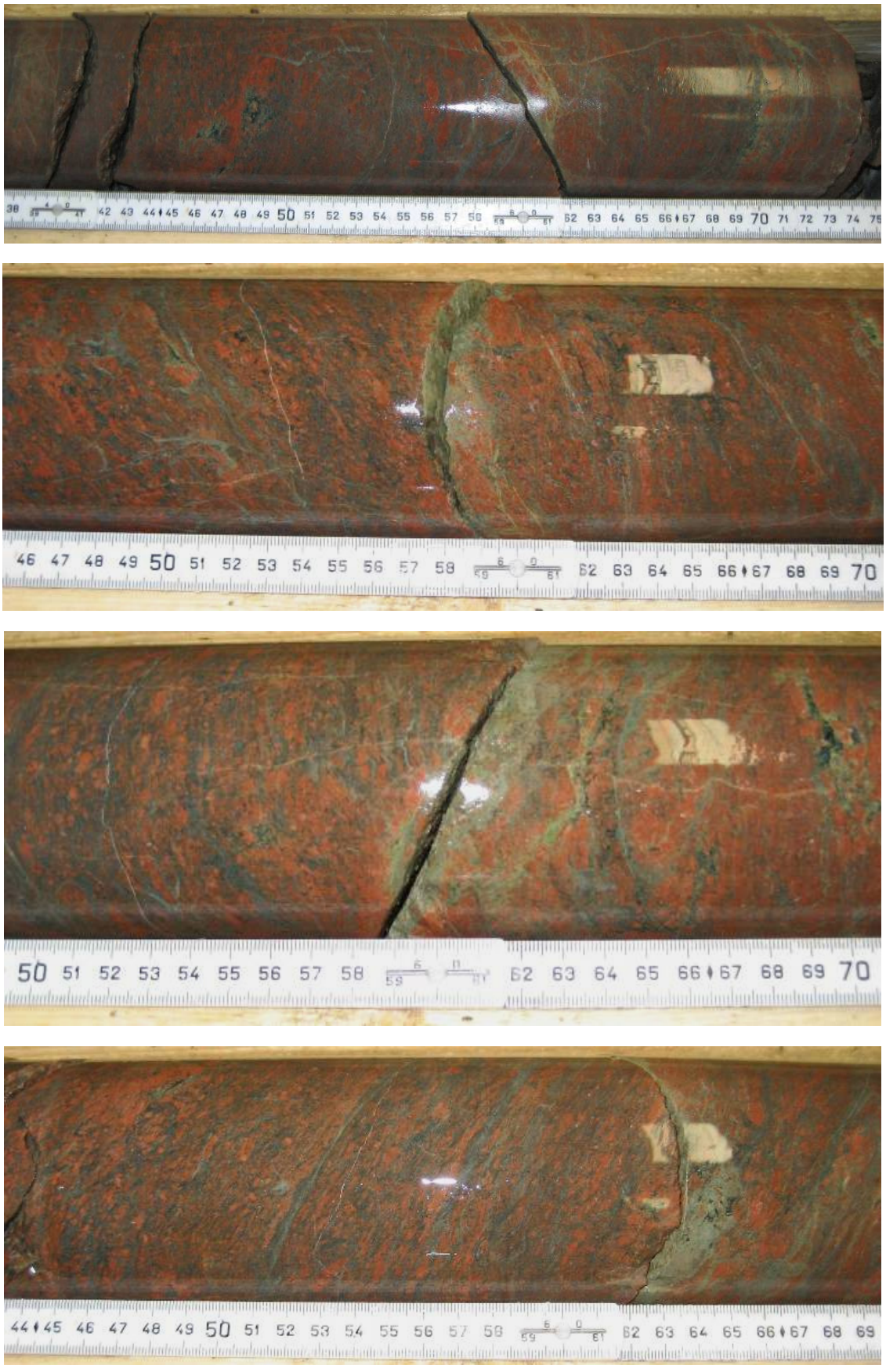

Figure 5–17. *Section containing 0.55-0.6 m from the core. In different rotation.*

Figure 5–18. *The fracture surface for the fracture at 0.592 m in the core. Dry and wet surface.*

In section 0.7-0.8 m the core was so broken that any rotation of the core would not supply the investigation with further information however, a rotation would rather cause the core to be more destroyed, therefore this was deferred from. Several fractures has been mapped in this section according to the geological mapping by Berglund /Jonsson et al., 2008/ and in the BIPS image there are two strong indications of opened fractures in this section (Appendix. A.2.). One of them, the fracture at 0.734 m, is seen as fracture 3 from the left in Figure 5-19. This fracture is described as filled with chlorite and calcite with a slight alteration (Figure 5-20) and its surface is rough and irregular.

Figure 5–19. *Section containing 0.7-0.8 m from the core.*

Figure 5–20. *The fracture surface for the fracture at 0.734 m in the core. Wet surface.*

The seismic investigation also indicates a fracture at about 1.20-1.25 m. In this section at 1.212 m, a fracture is found in the geological mapping and in the BIPS image of the borehole (Figure 5-21 and appendix A.2.). The fracture is filled with prehnite, chlorite and calcite and the fracture surface is slightly altered (Figure 5-22). In the geological mapping 12 opened fractures are found and five of them can be found as strong indications in the BIPS image. Of the five fractures indicated in the BIPS image and commented on as certain in the geological mapping, four are identified by the seismic investigation, (the fracture at 0.592 m in section 0.55-0.6 m, 0.763 m and 0.828 m in section 0.7-0.8 m and 1.212 in section 1.2-1.25 m).

Figure 5–21. *Section containing 1.2-1.25 m from the core. In different rotation.*

Figure 5–22. *The fracture surface for the fracture at 1.212 m in the core. Dry and wet surface.*

5.2.3 KQ0047A03

In this borehole an uncertain indication of a discontinuity has been identified at depth 1.55-1.65 m according to the seismic measurements. This uncertainty is because the response in the different parameters from the seismic investigation is quite ambiguous (Figure 5-23).

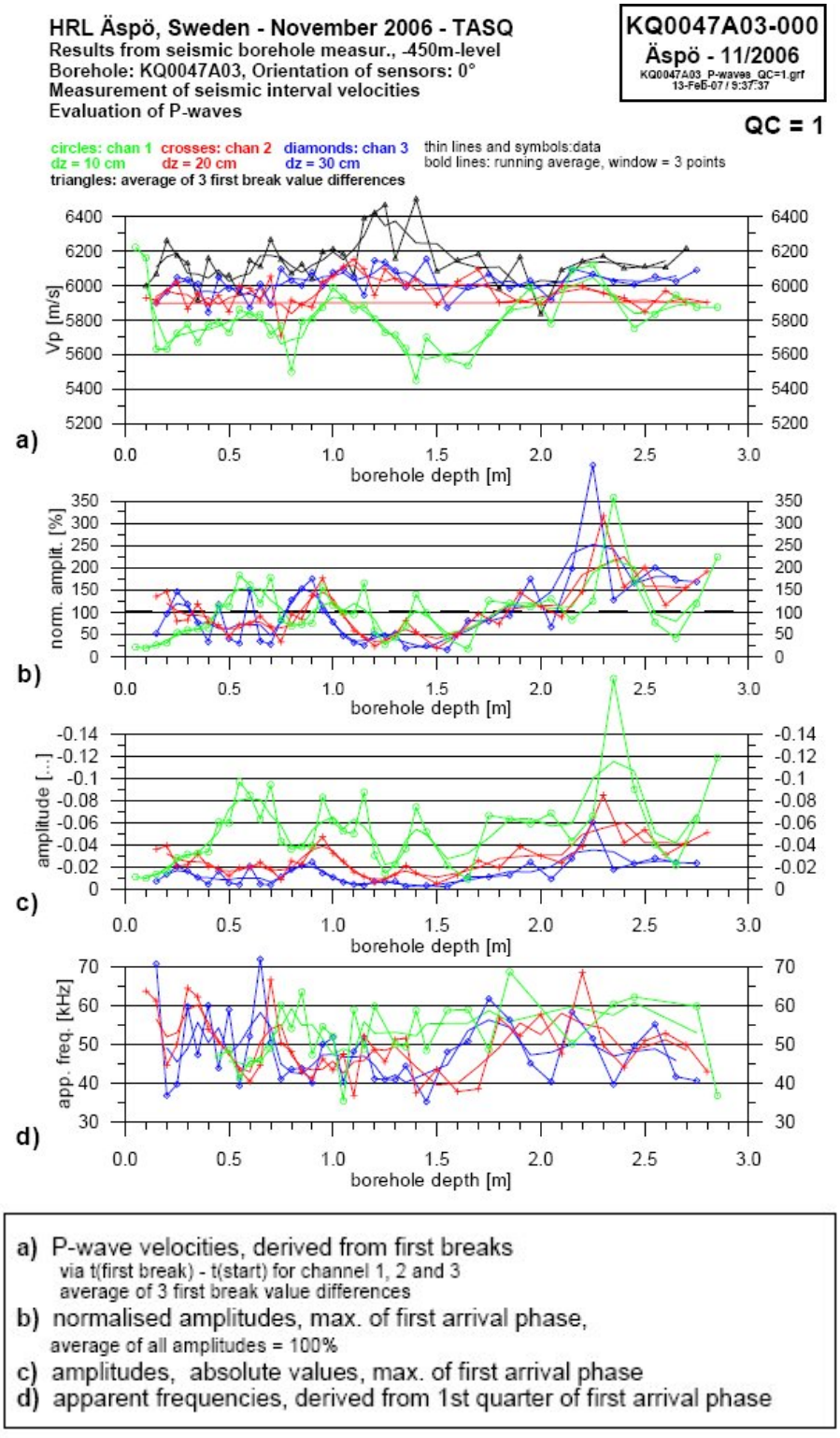

Figure 5–23. *The results from the seismic investigation of borehole KQ0047A02 /Schuster, 2007/.*

When investigating the core, the information from the mapping by Berglund /Jonsson et al., 2008/, indicates a total of 7 fractures where the core has been broken. There is an indication of a fracture at 1.991 m depth, but this distance is to far away from the area indicated to be considered as the source of the anomaly in the seismic measurements. At about 1.75 m depth, a change in rock type can be discerned as a dark band encircling the core. This contact is located at 0.1 m from the indicated section in the seismic measurements. The indication from the seismic measurements is commented as uncertain, and no fractures are found. A change of density at about this section is the only indication in the core that might be interpreted as the uncertain indication.

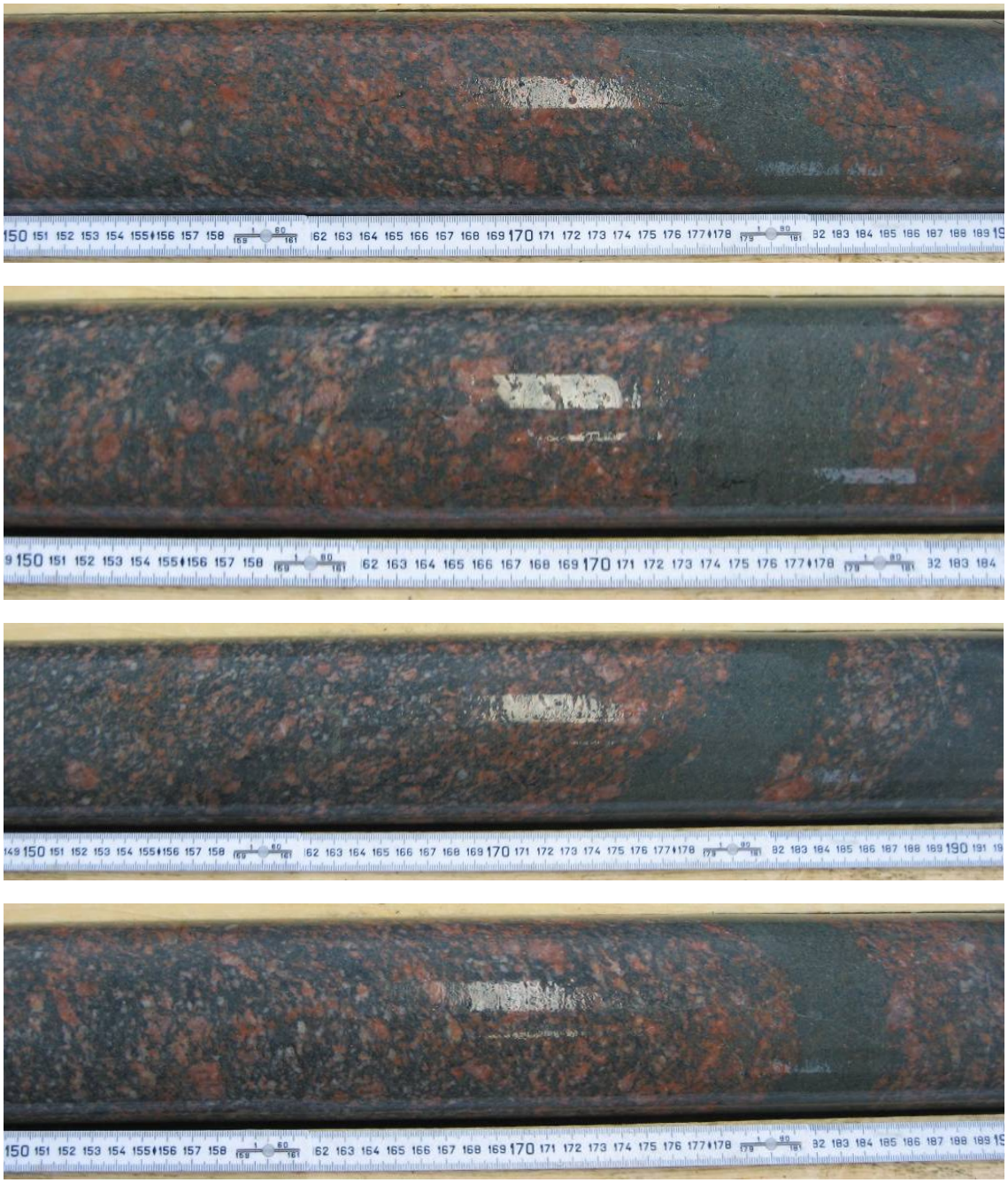

Figure 5–24. *Section containing 1.55-1.65 m from the core. In different rotation.*

5.2.4 KQ0047B01

In this borehole, no fractures have been indicated in the seismic investigation. No indication of open fractures could be found in the BIPS images (appendix A.4). From the geological mapping, 2 open fractures were identified, one as possible and one as probable by Berglund /Jonsson et al., 2008/.

5.2.5 KQ0047B02

In this borehole, no fractures have been indicated in the seismic investigation. No indication of open fractures could be found in the BIPS images (appendix A.5). From the geological mapping by Berglund, 12 open fractures were identified but none were commented as certain.

5.2.6 KQ0047G01

In this borehole the fractures are indicated at depth 0.4 m and uncertain fracture indications are found in the section 0.15-0.4 m and 2.05-2.15 m according to the seismic measurements (Figure 5-25).

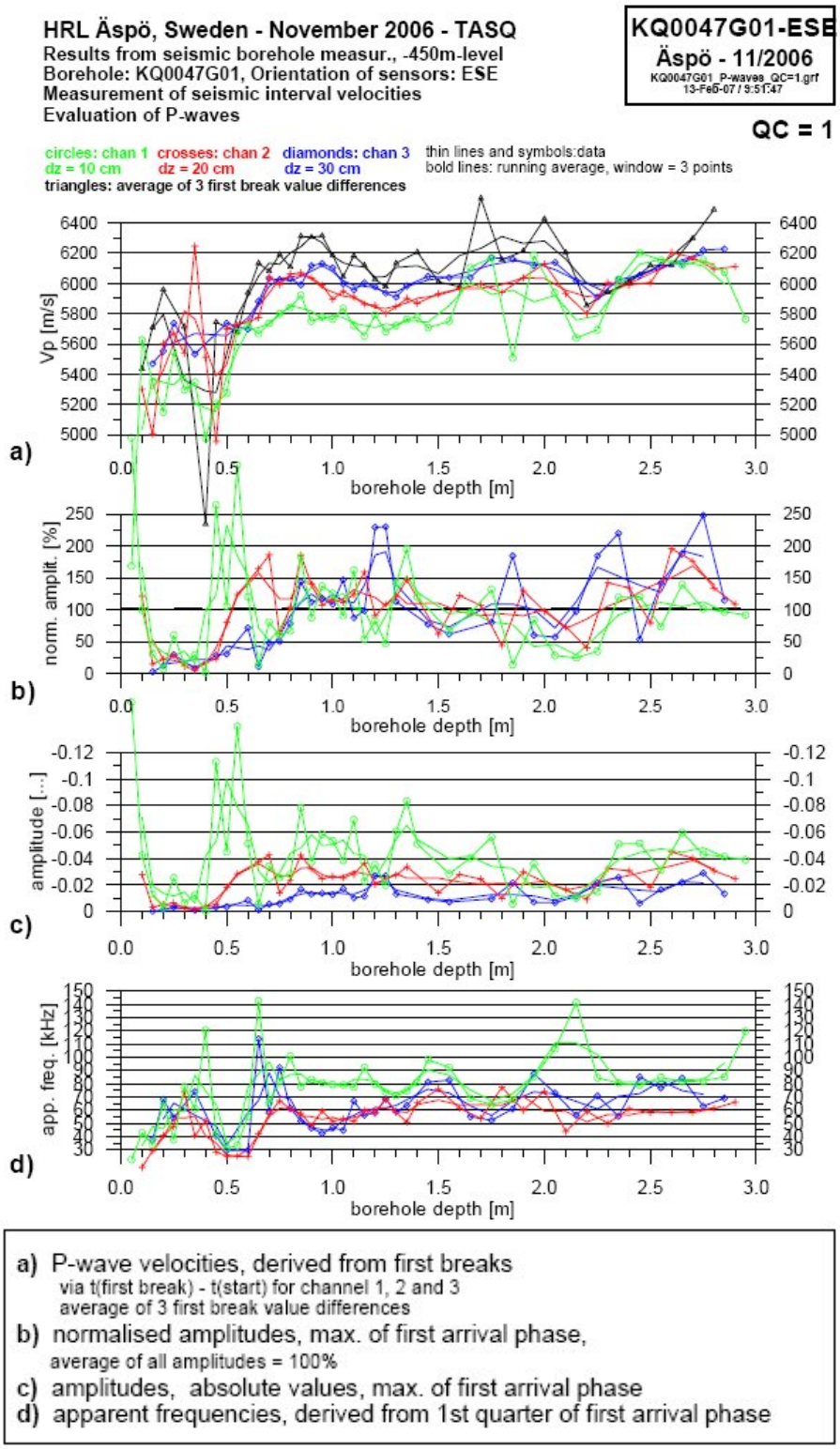

Figure 5–25. *The results from the seismic investigation of borehole KQ0047G01 /Schuster, 2007/.*

In the section at 0.15 m to 0.4 m there are 3 fractures indicated as opened in the geological mapping by Berglund /Jonsson et al., 2008/ which can be found in the BIPS image from the borehole (appendix A.6). These fractures are located at 0.209 m, 0.330 m and 0.394 m depth in the borehole (Figure 5-26). None of them have any fracture mineral, although their surfaces are slightly altered (Figure 5-27). The fracture indicated in the seismic measurement with certainty is at about 0.4 m depth which is consistent with the fracture at 0.394 m depth. The surface of this fracture can be seen in wet and dry condition in Figure 5-27

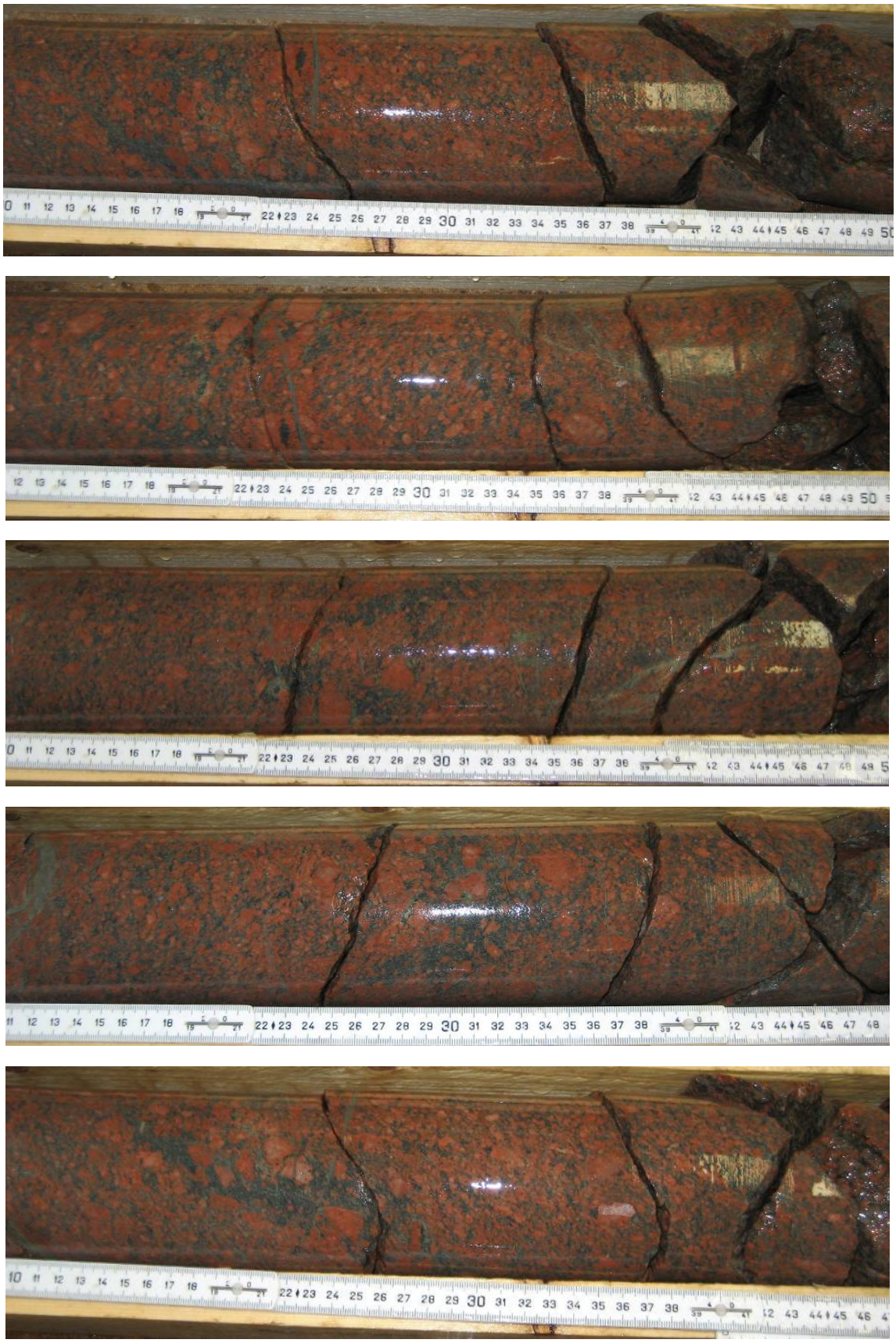

Figure 5–26. *Section containing 0.15-0.4 m from the core. In different rotation.*

Figure 5–27. *The fracture surface for the fracture at 0.394 m in the core. Dry and wet surface.*

The section containing the area indicated as uncertain fractures (2.05 m - 2.15 m) starts with a core break at about 2 m. However, no opened fractures are indicated either in the geological mapping by Berglund /Jonsson et al., 2008/ or in the BIPS image (Appendix A. 6.). It is in the closed fracture network containing chlorite that this core break occurs; the fracture network has a width in the core ranging from about 1 cm to 5 cm. This sealed fracture network can be the structural change that is indicated in the seismic measurements (Figure 5-28).

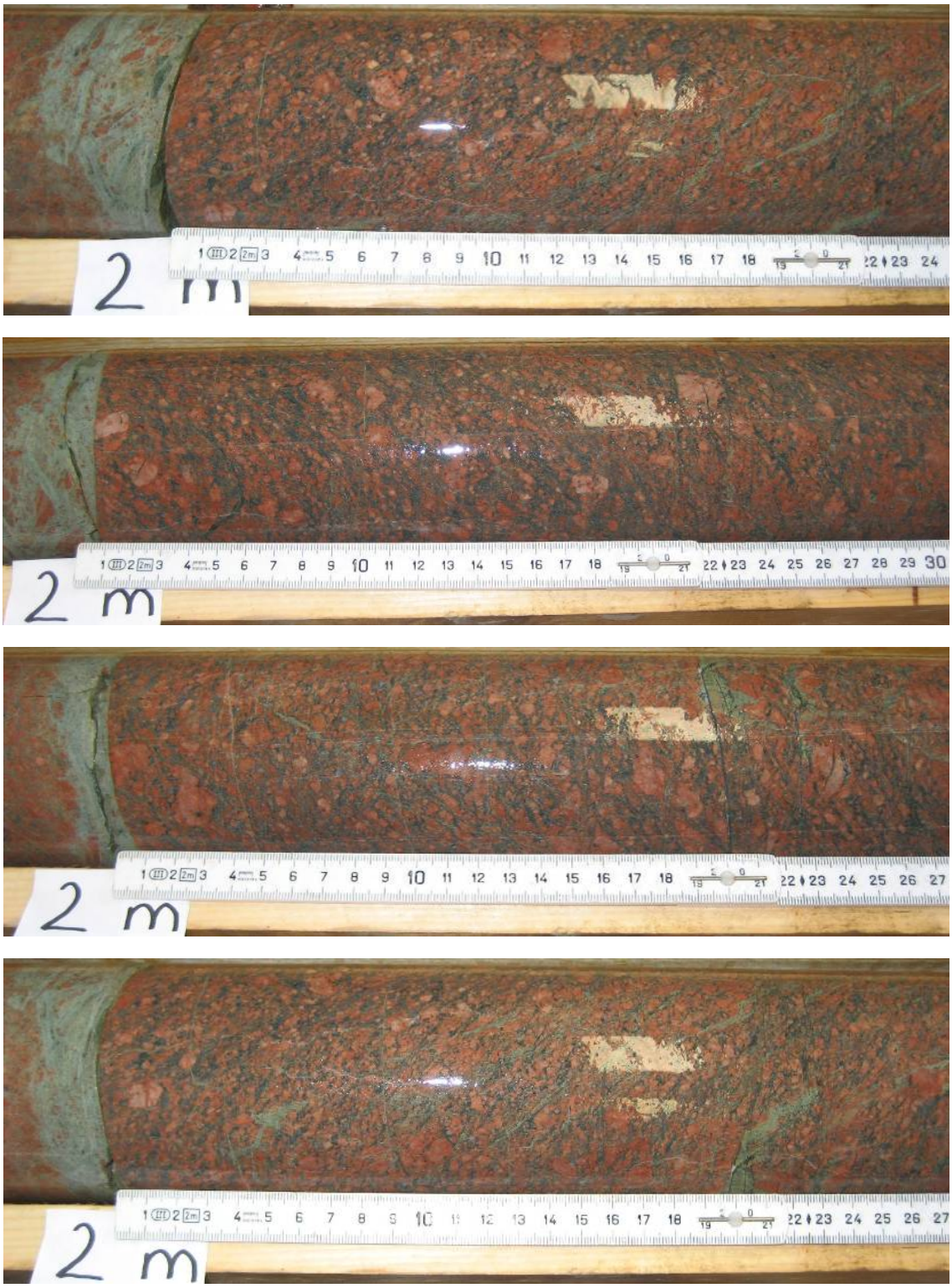

Figure 5–28. *Section containing 2.05-2.15 m from the core. In different rotation.*

5.2.7 KQ0047H01

In this borehole, two indications of uncertain fractures are found; one at depth 0.1-0.2 m and the other at 1.7 m. These indications are uncertain according to the parameters derived from the seismic measurements (Figure 5-29) and the seismograms.

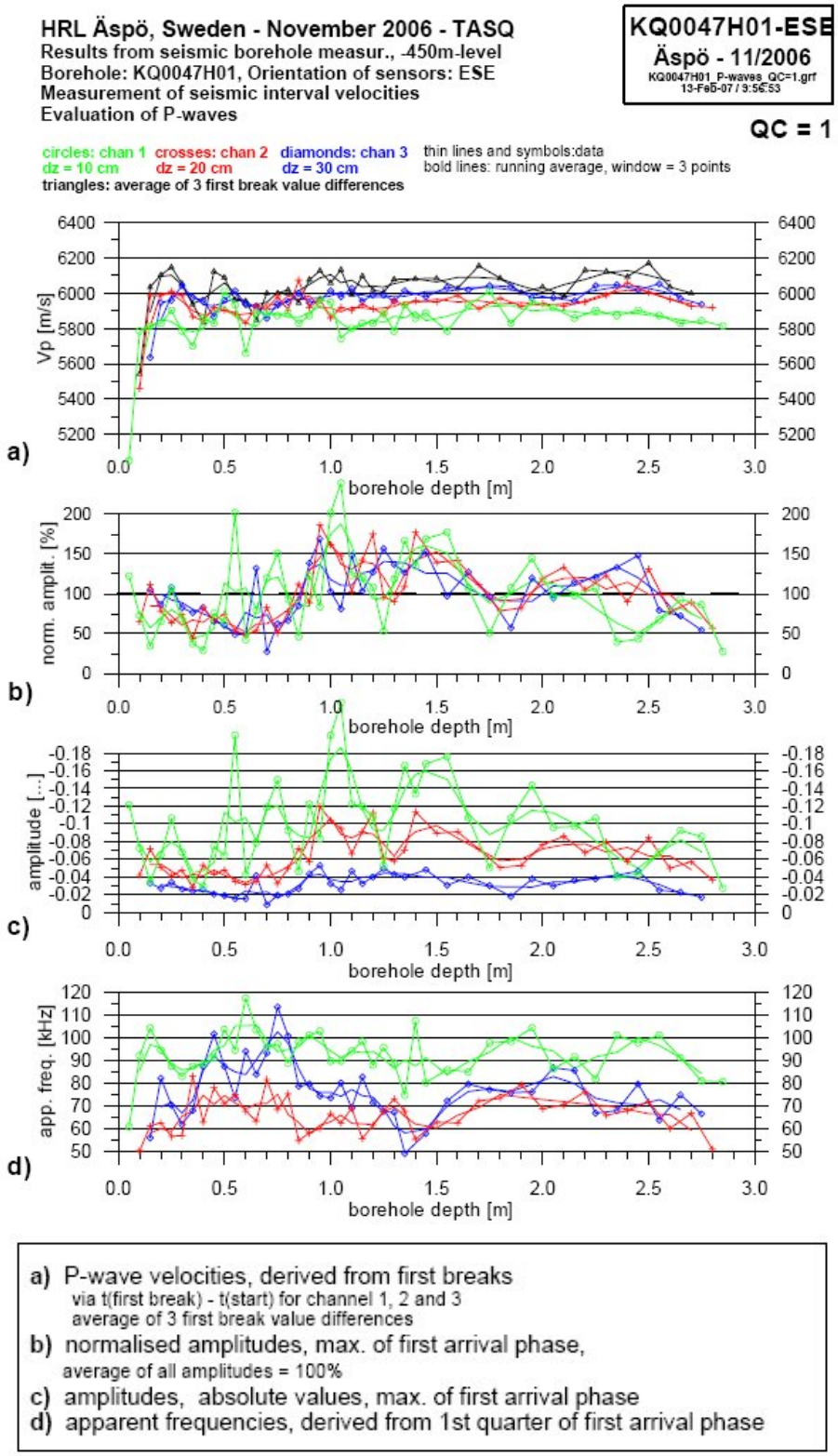

Figure 5–29. *The results from the seismic investigation of borehole KQ0047H01 /Schuster, 2007/.*

In the section between 0.1-0.2 m a fracture is found. The surface of this fracture which is located at 0.199 m, and seen in Figure 5-30, does not show any alteration. The main filling material in the fracture is chlorite according to the geological mapping. The surface of the fracture can be seen in Figure 5-31. This fracture cannot be identified in the BIPS image from the borehole, seen in appendix A. 7 and it is determined in the geological mapping as probable. The rock material in this section is quite variable from “low density” to “high density” minerals. This might have caused a mixed signal in the seismic record.

Figure 5–30. *Section containing 0.1-0.2 m from the core. In different rotation.*

Figure 5–31. *The fracture surface for the fracture at 0.199 m in the core. Dry and wet surface.*

In the section at 1.7 m depth in the borehole, an uncertain fracture indication is found in the seismic measurement. No fracture can be identified at this depth in the core or the BIPS image. The only structural indication in the core is an area with dark minerals, which indicate minerals with a higher density than the surrounding rock (Figure 5-32). This is similar to what has been identified in borehole KQ0047A03. In this core, the volume with the high density minerals can be found only in half the core profile. This implies that the indicators would not have been found if the probe were oriented in the opposite direction and not into the volume with high density minerals.

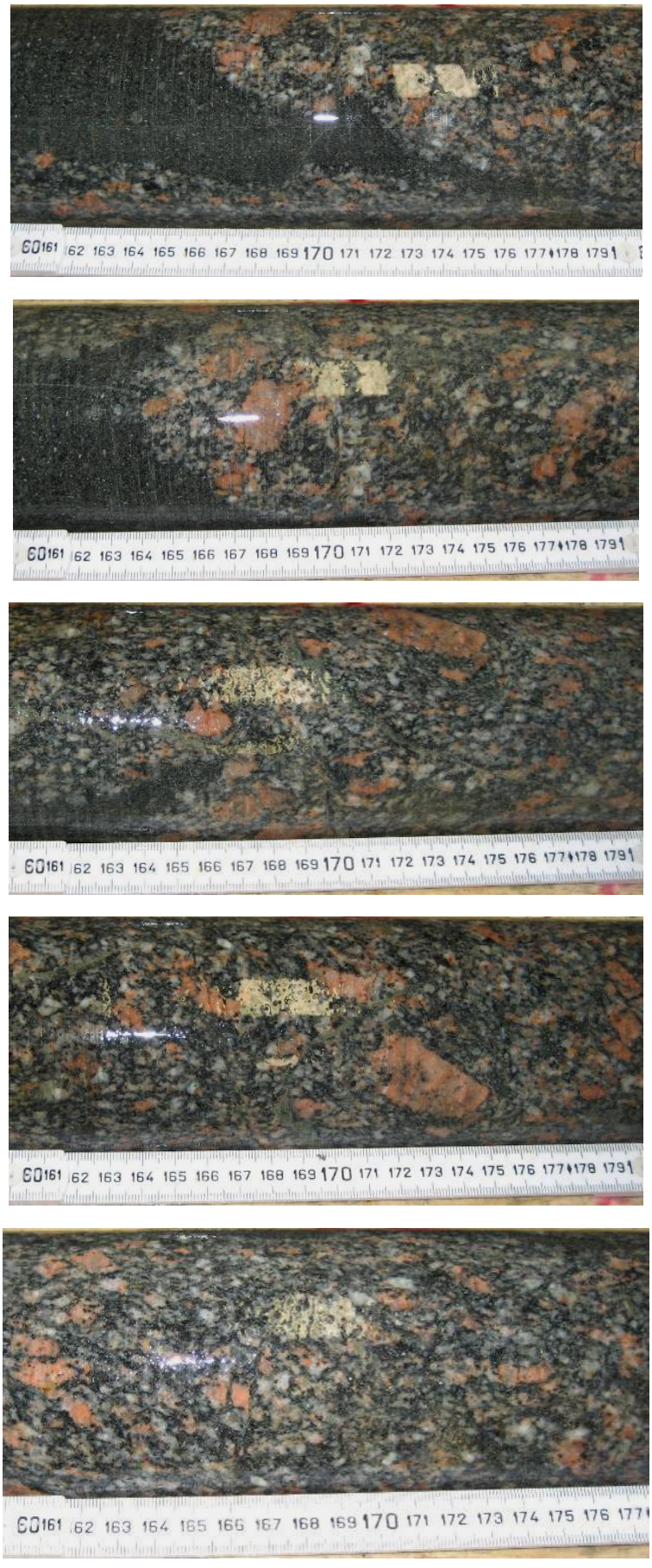

Figure 5–32. *Section containing 1.7 m from the core. In different rotation.*

5.2.8 KQ0047I01

In this borehole the possible fractures are indicated at depth 0.05-0.1 m and an uncertain possible fracture at 0.85-0.9 m according to the parameters derived from the seismic measurements (Figure 5-33) and the seismograms.

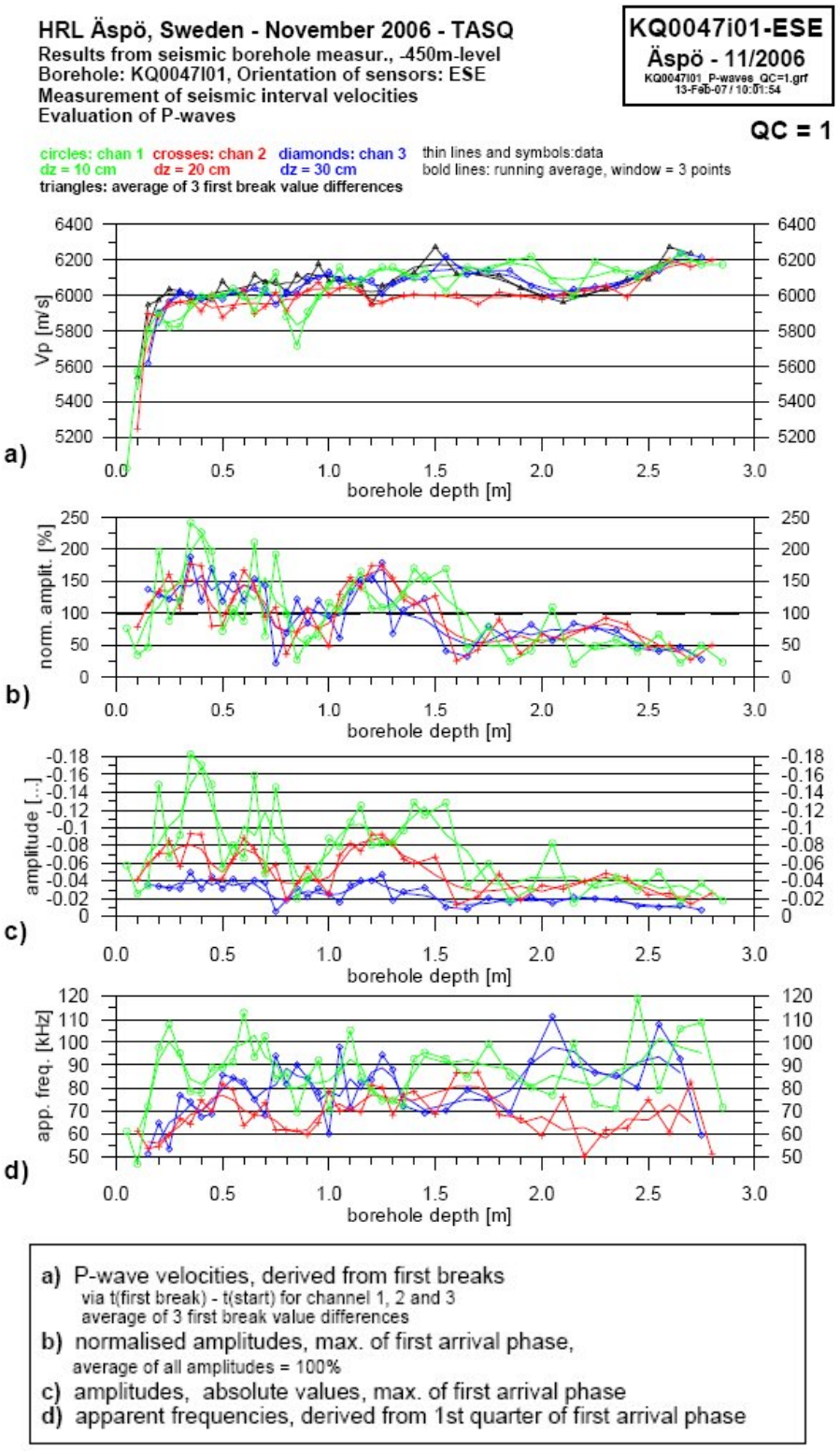

Figure 5–33. *The results from the seismic investigation of borehole KQ0047I01 /Schuster, 2007/.*

In the interval 0.05-0.1 m no fracture can be found but at 0.14 m a fracture with oxidized fracture surfaces can be found in the core by Berglund /Jonsson et al., 2008/. However, this fracture cannot be seen in the BIPS image (Figure 5-34), hence it is mapped as possible. Its surface is oxidized and irregular and can be seen in Figure 5-35.

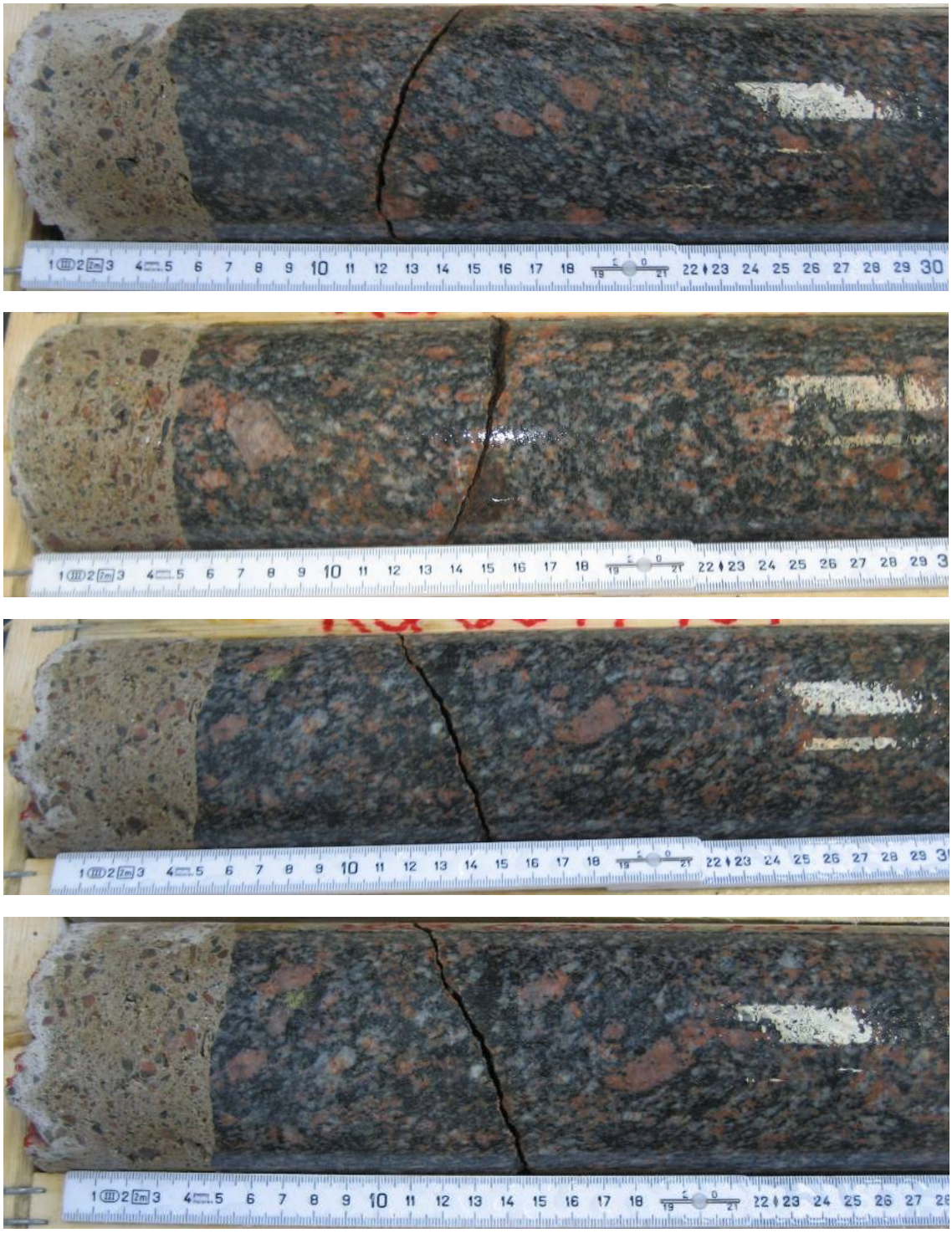

Figure 5–34. *Section containing 0.05-0.1 m from the core. In different rotation*

Figure 5–35. *The fracture surface for the fracture at 0.14 m in the core. Dry and wet surface.*

In the interval 0.85-0.9 m no open fracture is found in the geological mapping or on the BIPS image. The closest fracture is found in the core at 0.681 m. The quality of the BIPS image of this borehole is quite poor, which makes the identification of fractures difficult. No indication of a fracture in the BIPS image can be found at the depth of the fracture found in the core. As can be seen in Figure 5-36, a significant change in rock type occur at about 0.8-1.1 m. Depending on the location of the seismic measurement in the wall, this change in rock type could be the density change that the seismic measurement reacts to.

Figure 5–36. *Section containing 0.85-0.9 m from the core.*

5.2.9 Summary of the fracture indications and observations

In all the boreholes, fractures can be found in the geological mapping whereas in the BIPS images, not all the fractures can be observed. When fractures are observed both in the geological mapping and the BIPS they are referred to as certain. In this investigation the quality of the BIPS images were generally high with clear images of the borehole wall although for some of the boreholes the image quality is not so good (Appendix A.1.- A.8.). The seismic investigation have two different grades how well the fractures can be identified, certain and uncertain. The indication of an uncertain fracture is surrounded by brackets and followed by a question mark meanwhile the certain crack are indicated without brackets and question marks (Table 5.1). These indications are identified by the derived seismic parameter graphs as well as in the seismogram sections from the boreholes /Schuster, 2007/. A comparison of the existence of fractures obtained from the investigations using the drillcores and the investigation using the seismic investigation of the eight boreholes in the TASQ tunnel are given in Table 5-2.

Table 5-2. Identified fractures or other structural features that can be distinguished in the seismic interval velocity data as well as from the drillcores and the BIPS.

Borehole name	Suggested section with fractures from seismic (m)	Fractures indication in the drillcore and in BIPS (m)
KQ0047A01	0.20-0.25	0.248 -open in the core and visible in BIPS
KQ0047A01	0.7-0.75	0.743 –open fracture in the drillcore and visible in BIPS
KQ0047A02	0.55-0.6	0.592 -open in the core and visible in BIPS
	0.7-0.8	0.734 -open in the core and visible in BIPS (actually two fractures exist in this section)
	1.2-1.25	1.212 -open in the core and visible in BIPS
KQ0047A03	(1.55-1.65)?	No fracture found at this location but a change in mineral content can be observed in the core
KQ0047B01	No	No obvious open fracture indication found in the BIPS image from the borehole.
KQ0047B02	No	No obvious open fracture indication found in the BIPS image from the borehole.
KQ0047G01	(0.15-0.4)?	Several fractures found in both the core and BIPS.
	0.4	0.394 –open in the core and in BIPS
	(2.05-2.15)?	No fracture found at this location, however a closed fracture network containing chlorite is observed in the core.
KQ0047H01	(0.1-0.2)?	0.199 – open fracture in the core but not in BIPS
	(170)?	No fracture found at this location but a change in mineral content can be observed in the core.
KQ0047I01	(0.85-0.9)?	No fracture found at this location but a change in rock type can be observed in the core.

6 Rotational seismic measurements

In three boreholes; one in the side wall (KQ0047B01), one in the roof (KQ0047H01) and one in the floor (KQ0047G01) rotational measurements at different depth has been made (Figure 6-1). In each hole, the seismic array with the source and the three receiving channels were kept at one specific depth and rotated 360° in about 30° steps. This in order to identify how the seismic velocity varied in different direction. These measurements were made at different depth in the different holes. The locations of fractures and changes in geological structures crossing the borehole were avoided as much as possible. By identifying and avoiding changes in rock type and fractures in the drill core the optimal locations for these measurements were located.

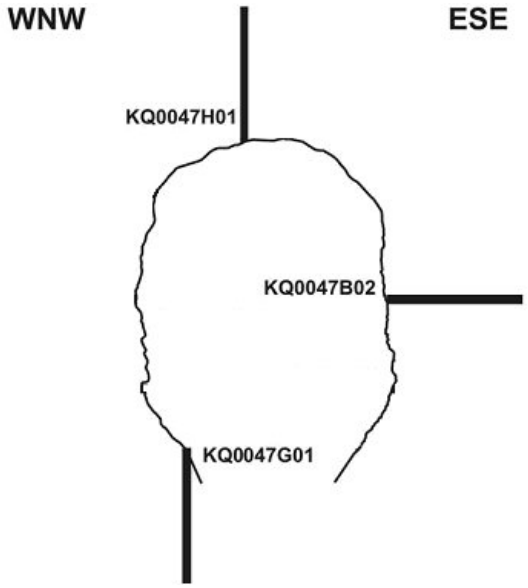

Figure 6–1. *Cross section of the TASQ tunnel and locations of the three boreholes in which the rotational investigation was conducted. The diameters of the boreholes are 92 mm. View from the entrance (SSW) towards the heading face of the tunnel (NNE).*

6.1 Rotational interval velocity measurements

For the seismic interval velocity measurements, the borehole probe is moved into the borehole along a certain orientation, e.g. at 12 o'clock position in the horizontal borehole.

In an isotropic or transversely anisotropic rock (and borehole orientation perpendicular to the bedding) all received signals are expected to be similar. However, in the case of seismic anisotropy, caused for example by stress redistribution in the rock this is not the case. Rotational measurements were therefore done in boreholes KQ0047H01, KQ0047G01 and KQ0047B02 at different depths as seen in Figure 6-2.

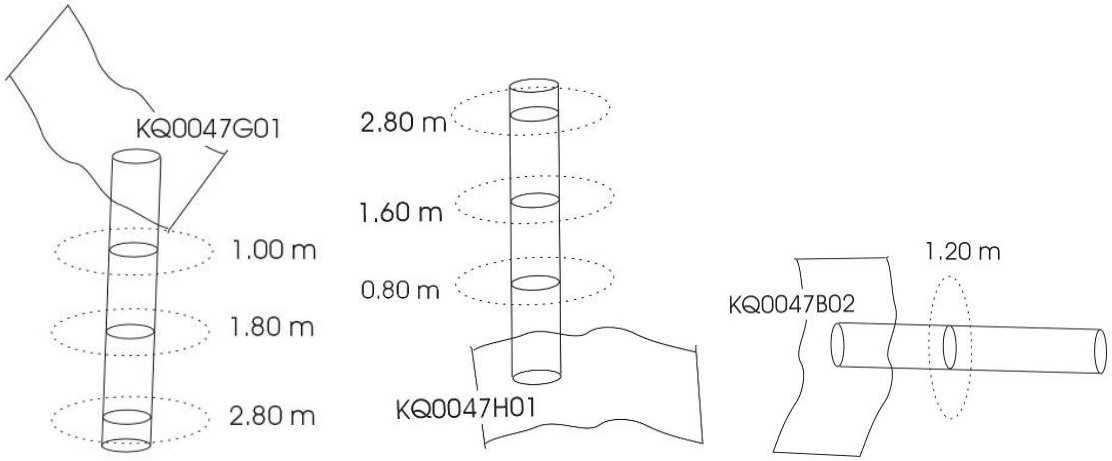

Figure 6–2. *Sketch of the rotational measurements performed in the three boreholes a) KQ0047G01, b) KQ0047H01, and c) KQ0047B02.*

6.2 Results from the rotational velocity measurements

The rotational measurements reported by Schuster /2007/ are reproduced here. The results obtained from the individual boreholes are presented in the sections below. The rotation angle of the two vertical boreholes in the floor and in the roof presented in /Schuster, 2007/ are defined in the way that 0 degree corresponds to the ESE wall. In order to compare the rotational measurements with other data given in this report, the directions of the rotational measurements have been transformed to the compass directions in this report. This transformation causes the first value measured to be plotted at 135° in the diagrams in Figure 6-3 and Figure 6-4. The seismic results used is the information from channel 3 (distance to source 0.3 m), measuring the largest volume of rock. In borehole KQ0047G01 (in the floor), the measurement at 0 and 360 degrees differ at all depth although in an ideal situation this cannot occur. This might be due to errors in the rotation angle during measurement, which is estimated to ±10° because the positioning in the vertical boreholes is done by visual judgement. The vertical measurement in the horizontal borehole in the wall started at the 12 o'clock position and was moved clockwise in the hole, this resulting in the tunnel axis to go through 90-270 degree in Figure 6-5. Also here the data from channel 3 is used. The positioning of the probe is much more accurate here (±1°) with the use of a positioning tool.

6.2.1 Results from KQ0047G01

The resulting P-wave velocity has been plotted on a circular diagram with the length of the bars indicating the velocities. As seen in Figure 6-3, the P-wave velocity is largest in the NE to the SW and smallest in the NW to SE direction. At 1 m depth, a strong anisotropy with highest velocity is found in the tunnel axis direction at this depth. The results at 1.8 m depth are quite scattered and non-uniform with the highest P-wave velocity to the W-SW and the lowest orthogonally to the E. The deepest measurement is rather isotropic, at 2.8 m depth. When investigating the velocities from different depth it can be seen that the velocities increase with increasing distance from the floor.

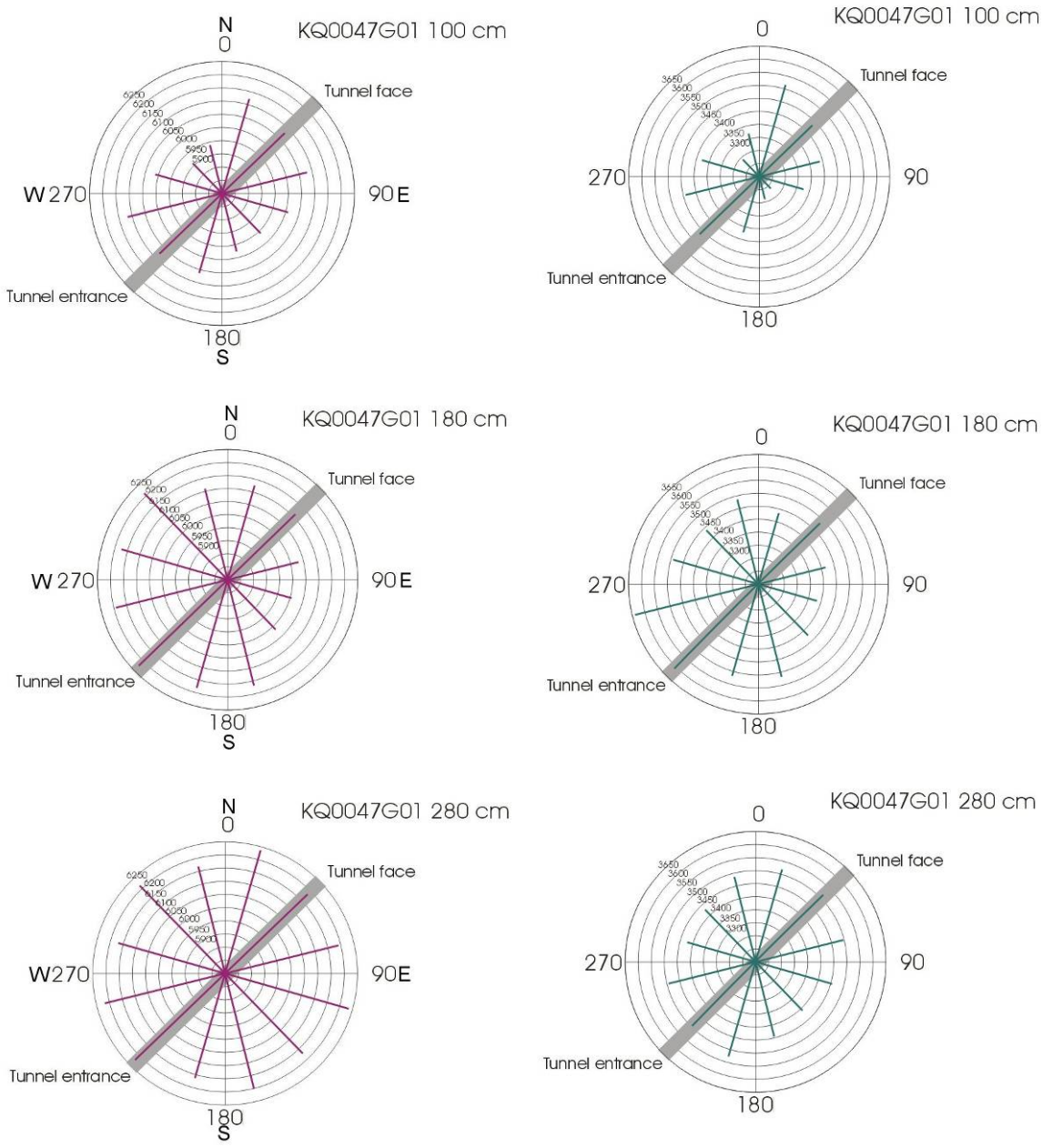

Figure 6–3. *Results from the velocity measurements in the borehole KQ0047G01 (in the floor) where the velocity is represented by bars in a 360° circular plot. The longer the bar the higher the velocity. Left: Compressional wave (P-wave) results. Right: Shear wave (S-wave) results .*

6.2.2 Results from KQ0047H01

Similar to the shallow measurement in borehole KQ0047G01, the P-wave velocity of the rotational measurement in the 0.8 m deep measurement of KQ0047H01 show a higher velocity in the NE-SW direction. This is the same direction as the tunnel axis. At a depth of 1.6 m, the P-wave velocity is non-uniform, however this measurement show a more pronounced 180°-perodicity than the measurement 1.8 m under the floor (Figure 6-3, middle). The highest velocity in the E-W direction is directed about 60° to the east compared to the highest velocity in the 0.8 m measurement. At largest depth in the roof (2.8 m) the P-wave velocity is quite homogenously dispersed although the velocity is generally lower at 2.8 m depth compared to 1.6 m. A very small velocity increase can be discerned in the ESE direction. This could indicate a rotation of the velocity as one move away from the tunnel into the rock mass.

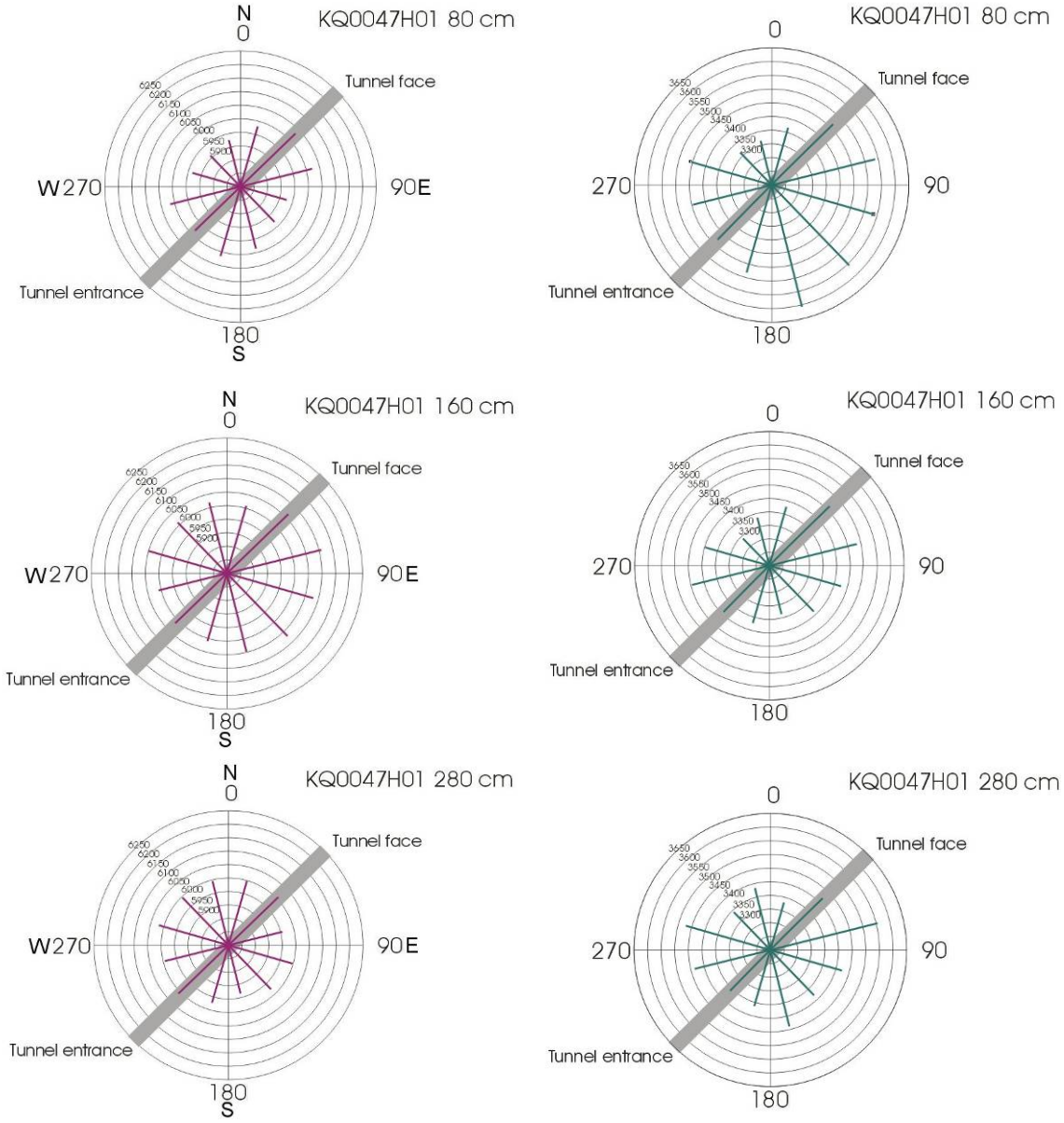

Figure 6–4. *Results from the velocity measurements in the borehole KQ0047H01 (in the roof) where the velocity is represented by bars in a 360° circular plot. The longer the bar the higher the velocity. Left: Compressional wave (P-wave) results. Right: Shear wave (S-wave) results .*

6.2.3 Results from KQ0047B02

This is a vertical measurement in the ESE wall of the tunnel at 1.2 m depth from the tunnel wall. Here the 0 is in the up-wards direction. In this borehole only one rotational measurement was performed. This measurement indicates a high disparity in different directions which does not indicate any preferred direction of velocity increase. This disparity prevents any conclusions of this measurement.

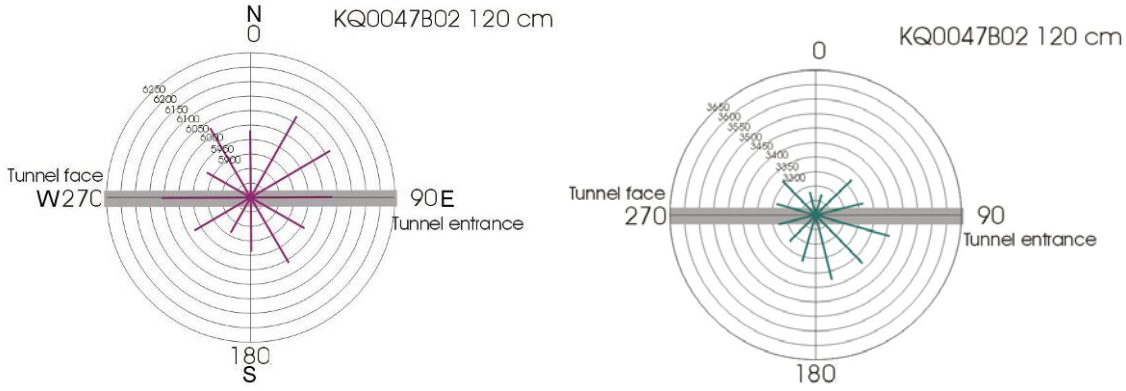

Figure 6–5. *Results from the velocity measurements in the borehole KQ0047B02 (in the ESE wall) where the velocity is represented by bars in a 360° circular plot. The longer the bar the higher the velocity. Left: Compressional wave (P-wave) results. Right: Shear wave (S-wave) results .*

7 Discussion

As seen in this investigation, the identification of fractures in crystalline rock in the vicinity of a tunnel can be made using the ultrasonic method. The fractures identified in the seismic investigation have all been identified in the borehole (in the BIPS image) and in the core. This method identifies structures that cross the borehole. As the probe passes the fracture, the change in elastic properties gives different responses. However, the response depends on the relation between the orientation of the structure and the orientation of the borehole. If the angle between the borehole axis and the structure is high, the response is abrupt whereas in the case of sub-parallel structures, the response is more gradual /Lowrie, 1997/. As the transmission and the reflection coefficient of the interface affect the amplitude of the recorded seismic waves it should be possible to distinguish between fractures and changes in rock type. In this investigation both fractures and changes in rock type has been identified. Fractures are distinguished as more abrupt changes in the ultra sonic wave propagation (indicated as certain in the seismic investigation). The changes in rock type have been identified as less distinct changes in the ultra sonic wave propagation (indicated as uncertain in the seismic investigation).

The change in elastic properties when changing rock type gives a response in the elastic properties that is less abrupt than fractures. This method measures the seismic wave velocity in a small volume of rock along the borehole which accentuates abrupt changes in the elastic properties such as fractures compared to measurements that measure the elastic properties over larger volumes in which the fracture response are more “blurred”. The uncertain indications of fractures could have been a response of fractures with a sub-parallel orientation to the borehole but in this case it is found that they are indications of rock type changes, or similar structures as chlorite filled zones. The uncertain indications are less abrupt than the certain indications in the seismic measurements and this gives a possibility to divert between fractures and changes in density due to variation in rock type. In a volume where the elastic properties already are subject to damage - like in the excavation damage zone surrounding the tunnel, the indication of a single fracture in the seismic record will be uncertain.

The seismic wave velocity depends on changes in the rock mass such as; the geological structures encountered along the borehole, the stress situation around the borehole and water content in the rock etc. A rock type with a higher density will cause the P-wave velocity to increase, just as lower density rocks as well as fractures will cause the P-wave velocity to decrease /Lowrie, 1997/. S-waves cannot travel through water which will cause the S-wave velocity to be more sensitive to the occurrence of water. Close to a large drain such as a tunnel or the borehole, the S-wave measurements will be more reliable due to the lack of water in the rock. As the wavelength for S-waves are shorter for S-waves their spatial resolution is higher. The stress situation on the rock mass will adapt to the free surface of the borehole but especially around the tunnel which will have a large effect on the velocity. The orientation of the tunnel amplifies the stress situation in the vertical boreholes, thus the P-wave and S-wave minima can be seen in the direction of the maximum far-field stress. Although the TASQ tunnel was built with the stress situation in mind a small misalignment of the tunnel-axis to the principal stress tensor can be seen in the ultrasonic measurements from boreholes KQ0047G01

and KQ0047H01. For KQ0047G01, seen in Figure 6-3, the P-wave and S-wave velocity is largest in the NE to the SW and smallest in the NW to SE direction at shallow depths similar to the results in the roof (KQ0047H01). The results for KQ0047G01 at 1.8 m depth are quite scattered and non-uniform with the highest P-wave velocity to the W-SW and the lowest orthogonally to the E. The deepest measurement is rather isotropic, at 2.8 m depth in both the roof and the floor. Both here and in the measurements in the roof the response to the stress field is more pronounced in the S-wave velocity. The S-wave shows a minimum in the maximum principal stress direction. The third major cause of changes in the P-wave velocity is the structures around the borehole measured. When measuring the rotational interval measurement sequences of the borehole without fractures and changes in rock type, were used. This leaves the water content and the stress situation to affect the measurements. The water content in the holes is strongly depending on the fractures in crystalline rock and away from them the dry zone around the tunnel and the boreholes develop quite isotropically out from the structure. This leaves the effect of the stress situation on the P-wave and S-wave velocity. In the measurements in the floor (Borehole KQ0047G01) the general trend is that the P-wave velocities increase as the measurement probe moves away from the tunnel but this trend can not be seen in the roof (borehole KQ0047H01), where the P-wave velocity is lower in the 2.8 m deep measurement compared to the measurement at 1.6 m depth from the tunnel. In both the P-wave and S-wave velocity an effect of the tunnel can be seen in both borehole KQ0047G01 and KQ0047H01. In the measurements furthers out from the tunnel a stronger response to the far-field stress can be seen in the S-wave velocity than the P-wave velocity.

8 Conclusions

In this study it has been found that the certain indications of fractures in the ultrasonic measurements are possible in the rock type found in the TASQ tunnel. The uncertain indications are more likely to indicate changes in the density of the rock material, if the indication are not within the EDZ where the distinction of single fractures are disrupted by the general damage found in the rock mass.

From the rotational measurements it is found that the effect of the tunnel amplifies the general effect of the far-field stress situation close to the structure and can be identified in the P-wave and S-wave velocity out to about 1 m from the tunnel. Further out from the tunnel the velocity maxima start to rotate compared to the tunnel-axis which indicate a small deviation of the tunnel alignment to the general stress field. Even at large a large distance to the tunnel the response to the far-field can be found in the S-wave.

This is a verification of the results found for the stress situation, fractures and changes in rock type in an ultrasonic investigation of the EDZ. Further investigations of the effect of the stress situation on the ultrasonic wave velocity around tunnels in this type of rock are recommended. A first step in that direction is to model the stress situation around the tunnel, including the information of the fracture network and geometry of the built tunnel.

9 References

Autio, J. 1997. Characterization of the excavation disturbance caused by boring of the experimental full scale deposition holes in the Research Tunnel at Olkiluoto. Svensk kärnbränslehantering ABTecnical report. 97-24. 118.

Borm, G., Giese, R., Otto, P., Amberg, F., Dickmann, Th. 2003. Intergrated Seismic Imaging System for Geological Prediction during Tunnel construction. ISRM 2003 - Technology roadmap for rock mechanics, South African Institute of Mining and Metallugy. 5.

Cardarelli E. Marrone C. Orlando L. 2003. Evaluation of tunnel stability using intergrated geophysical methods. Journal of Applied Geophysics. 52. 93-102.

Carlson S. R. Young R. P. 1993. Acoustic Emission and Ultrasonic Velocity Study of Excavation-Induced Microcrack Damage at the Underground Research Laboratory. International Journal of Rock Mechanics & Mining Sciences. 30. 901-907.

Hirahara N. Ishihara T. Maeda N. Sugihara K. Sato T. 1999. In-situ experiment on effect of excavation method on excavation disturbance at the Tono mine in Japan. Radioactive Waste Management and Environmental Remediation – ASME. 8.

Jonsson M, Berglund J, Bäckström A, Feng Q, Mas Ivars D, Johansson M, Olsson M. 2008. SAFEDZ – Summary and Analyisi of Factors that affect and control the Excavation Disturbance/Deformation Zone. SKB report in prep. Svensk Kärnbränslehantering AB. 118.

Klose CD. Loew S. Giese R. Borm G. 2007. Spatial predictions of geological rock mass properties based on in-situ interpretations of multi-dimensional seismic data. Engineering Geology. 93. 99-116.

Lowrie W. 1997. Fundamentals of Geophysics. Cambridge University Press. Cambridge. 354.

Schuster K. 2007. Äspö Hard Rock Laboratory, DECOVALEX; Ultrasonic borehole measurements in the TASQ tunnel (450 m level) at Äspö HRL performed by BGR in November 2006. SKB IPR-07-08, Svensk Kärnbränslehantering AB. 118.

Schuster K. Alheid H.-J. 2002. Engineered Barrier (EB) Experiment and Geophysical Characterisation of the Excavation Disturbed Zone (ED-C) Experiment: Seismic Investigation of the EDZ in the EB niche. - Mont Terri Technical Report TR 02-03, swisstopo, Wabern, Switzerland.

SICADA, 2007-06-19. Tables with information of fracture mapping of boreholes KQ0047A01, KQ0047A02, KQ0047B01, KQ0047B02, KQ0047G01, KQ0047H01 and KQ0047I01.

Zimmerman RW. King MS. 1985. Propagation of acoustic waves through cracked rock. 26th US Symposium on Rock Mechanics. 739-745.

Appendix A

This Appendix contains the BIPS images for the different boreholes, were the markings to the left of the core is in meters.

A.1. KQ0047A01


D L U R D
1,120
1,160
1,200
1,240
1,280
1,320
1,360
1,400
1,440
1,480
1,520
1,560
1,600
1,640
1,680
1,720
D L U R D
1,680
1,720
1,760
1,800
1,840
1,880
1,920
1,960
2,000
2,040
2,080
2,120
2,160
2,200
2,240
2,280

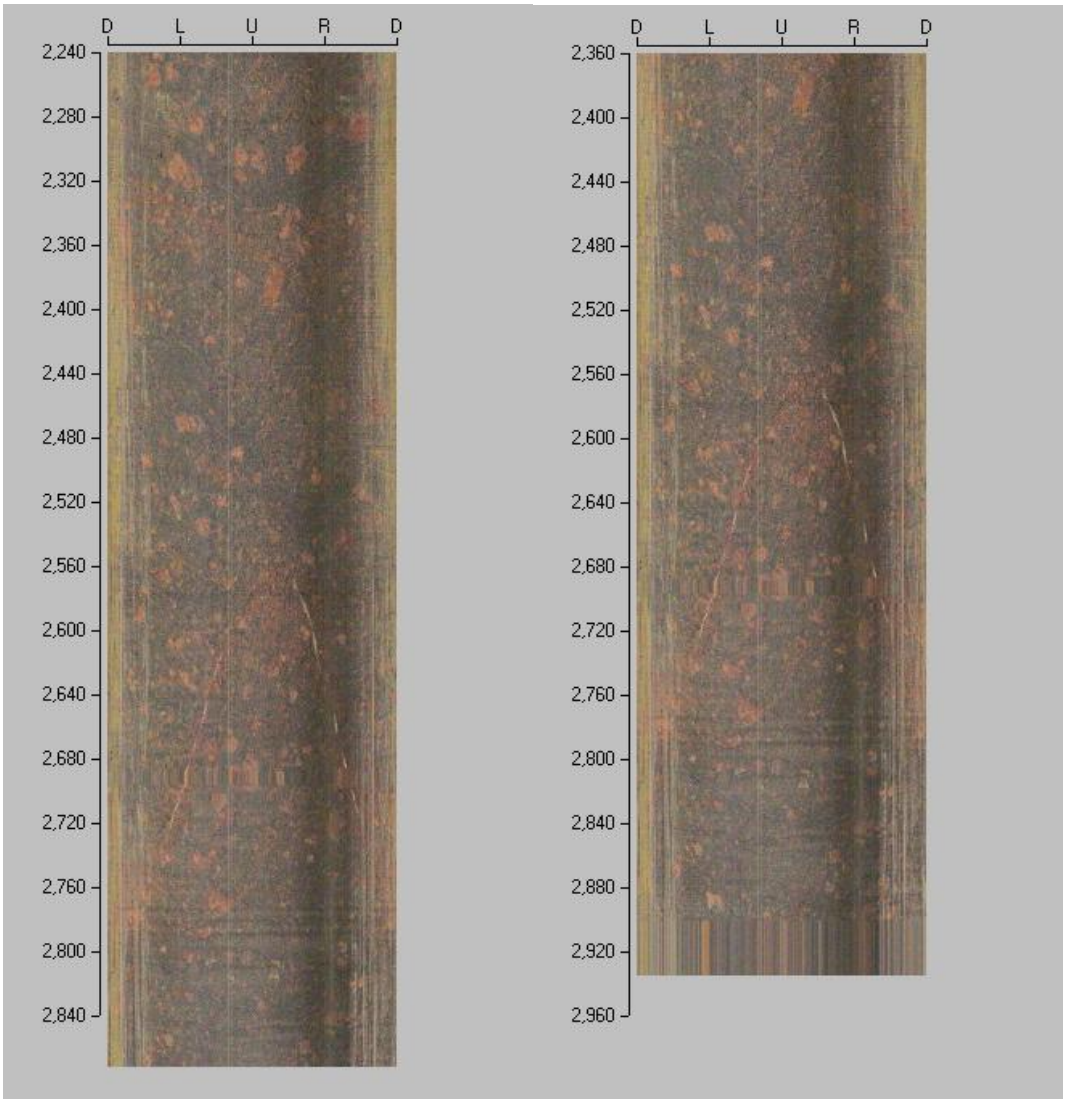
D L U R D
2,240
2,280
2,320
2,360
2,400
2,440
2,480
2,520
2,560
2,600
2,640
2,680
2,720
2,760
2,800
2,840
D L U R D
2,360
2,400
2,440
2,480
2,520
2,560
2,600
2,640
2,680
2,720
2,760
2,800
2,840
2,880
2,920
2,960

A.2. KQ0047A02

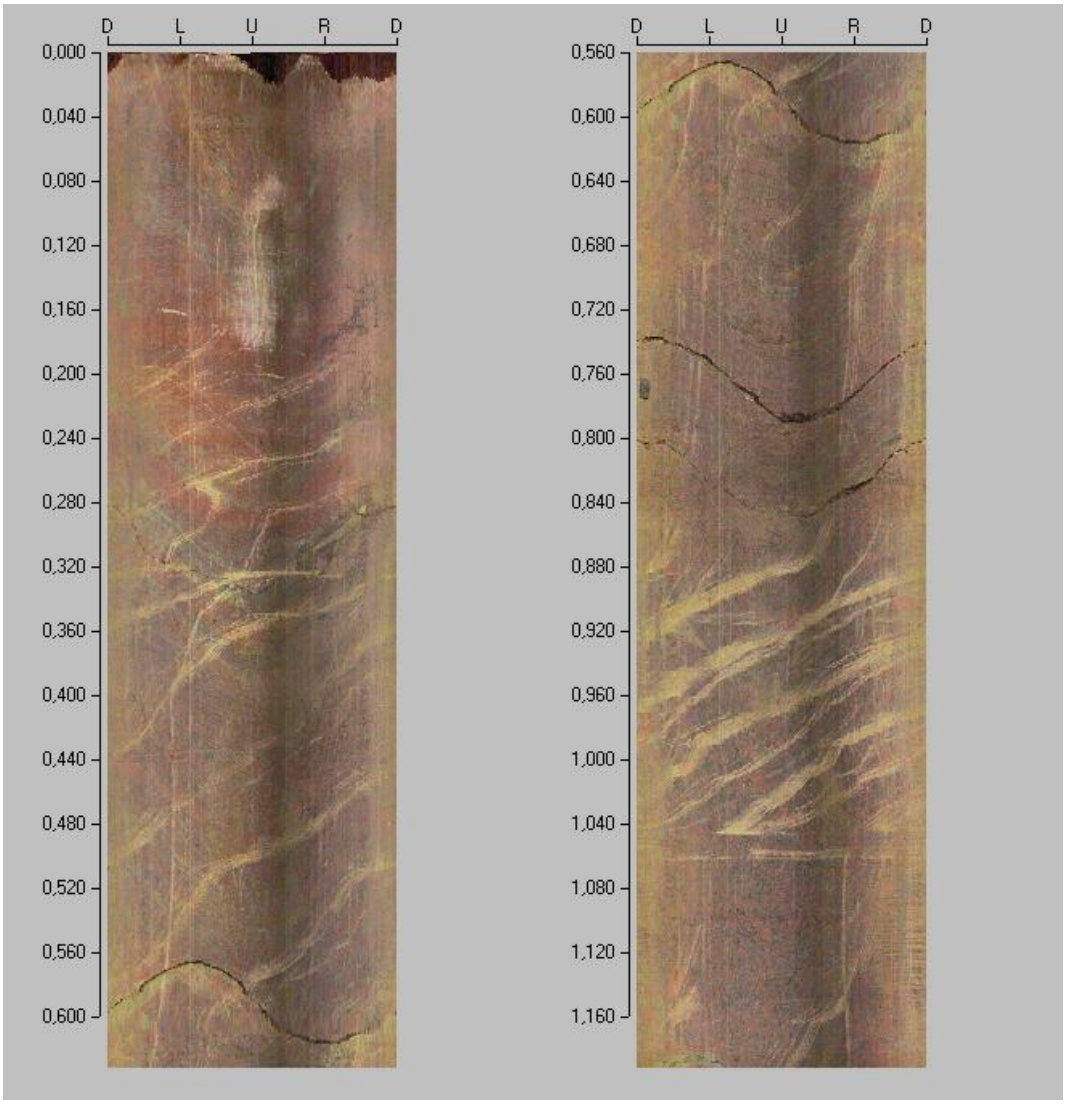

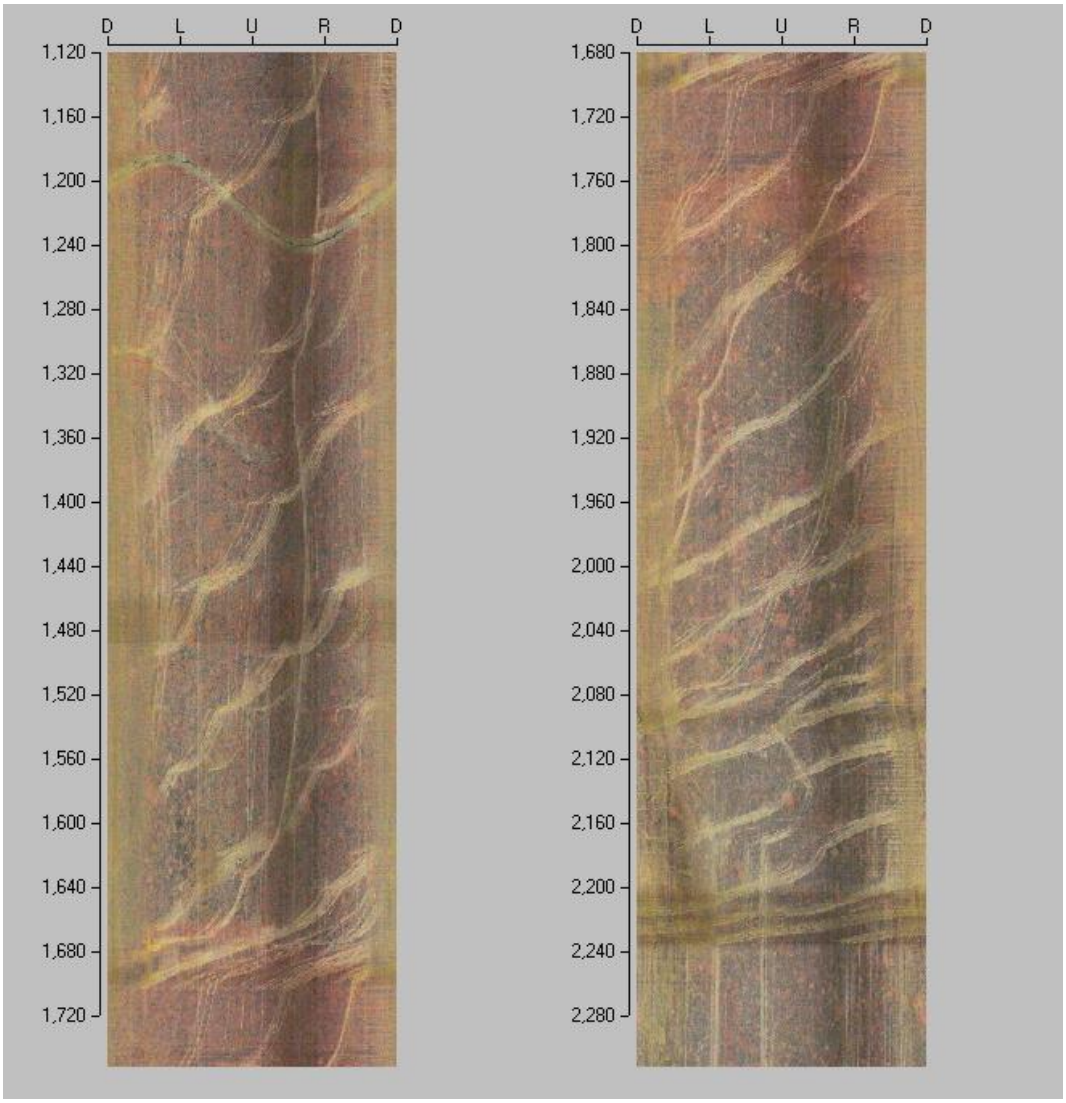
D L U R D
1,120
1,160
1,200
1,240
1,280
1,320
1,360
1,400
1,440
1,480
1,520
1,560
1,600
1,640
1,680
1,720
D L U R D
1,680
1,720
1,760
1,800
1,840
1,880
1,920
1,960
2,000
2,040
2,080
2,120
2,160
2,200
2,240
2,280

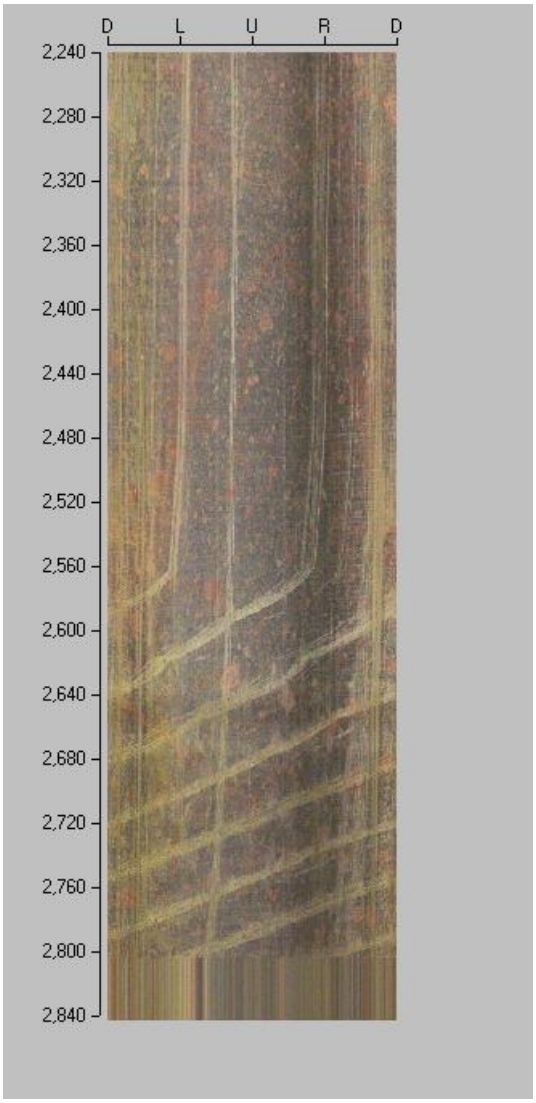
D
L
U
R
D
2,240
2,280
2,320
2,360
2,400
2,440
2,480
2,520
2,560
2,600
2,640
2,680
2,720
2,760
2,800
2,840

A.3. KQ0047A03

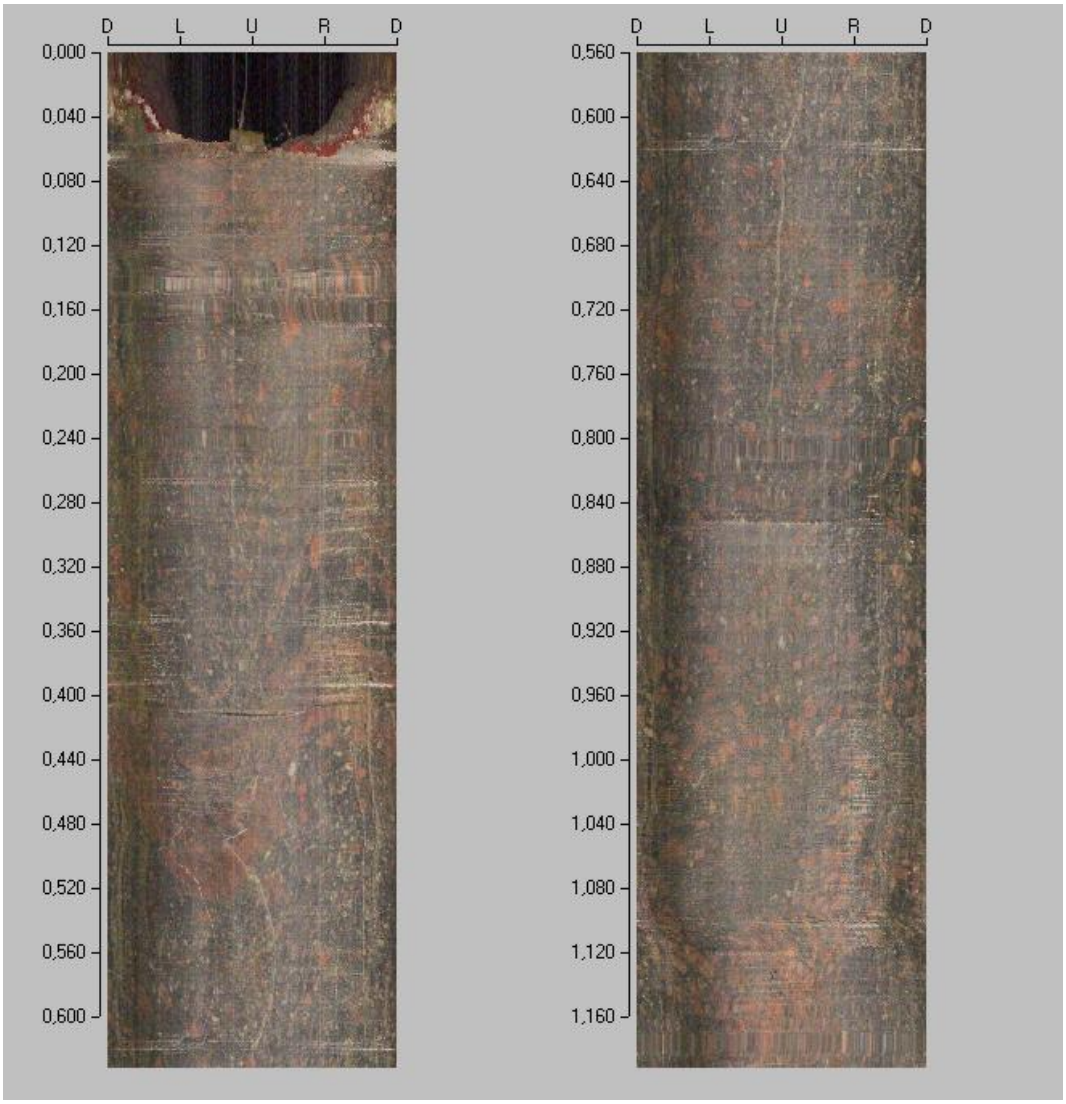


D L U R D
1,120
1,160
1,200
1,240
1,280
1,320
1,360
1,400
1,440
1,480
1,520
1,560
1,600
1,640
1,680
1,720
D L U R D
1,680
1,720
1,760
1,800
1,840
1,880
1,920
1,960
2,000
2,040
2,080
2,120
2,160
2,200
2,240
2,280

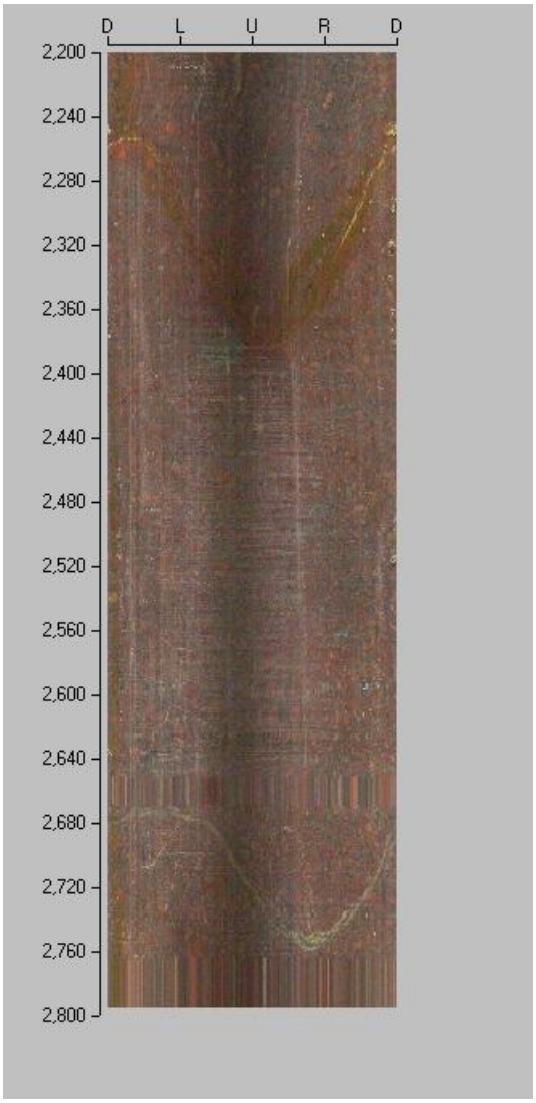
D
L
U
R
D
2,200
2,240
2,280
2,320
2,360
2,400
2,440
2,480
2,520
2,560
2,600
2,640
2,680
2,720
2,760
2,800

A.4. KQ0047B01

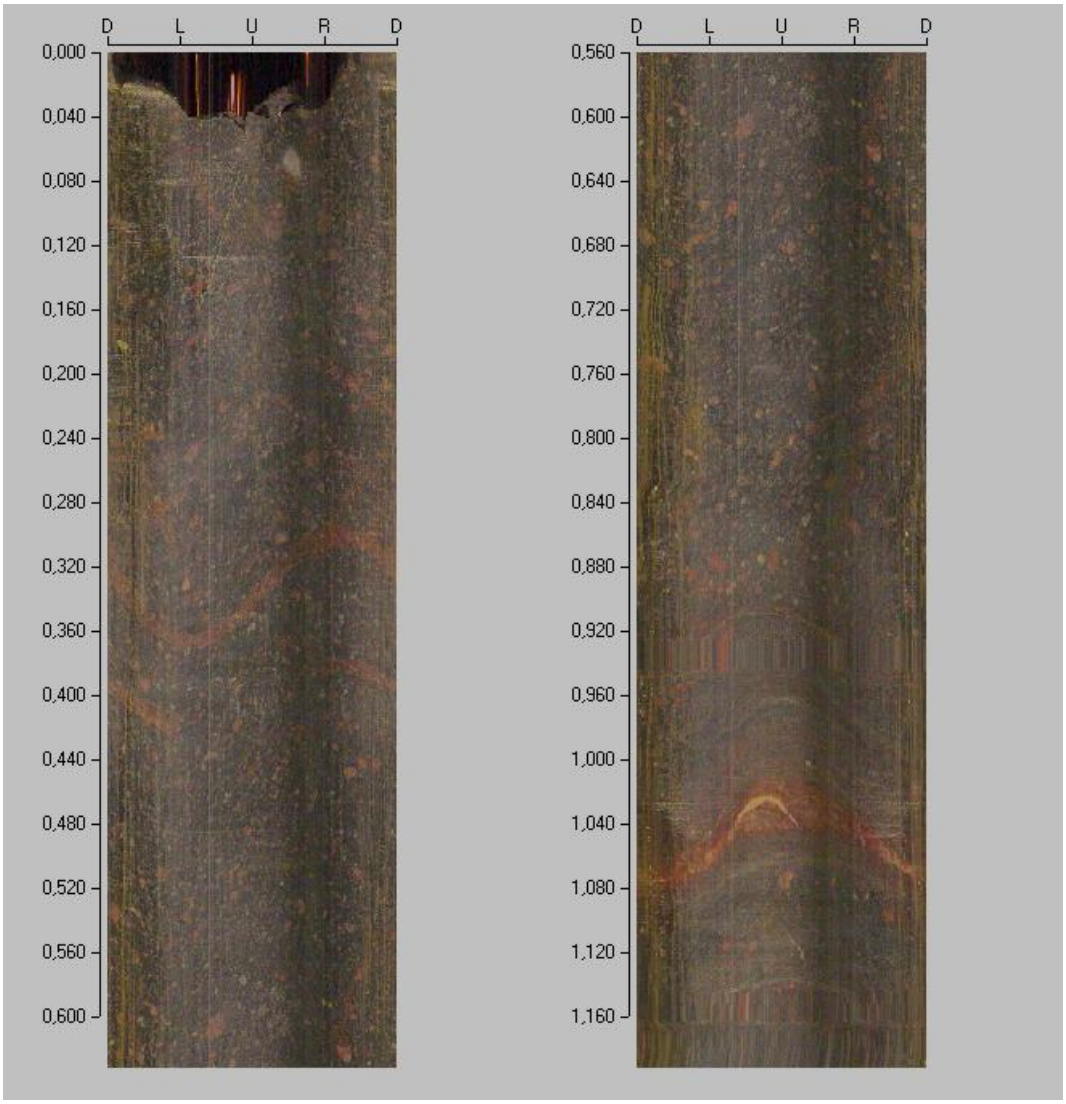


D L U R D
1,120
1,160
1,200
1,240
1,280
1,320
1,360
1,400
1,440
1,480
1,520
1,560
1,600
1,640
1,680
1,720
D L U R D
1,680
1,720
1,760
1,800
1,840
1,880
1,920
1,960
2,000
2,040
2,080
2,120
2,160
2,200
2,240
2,280

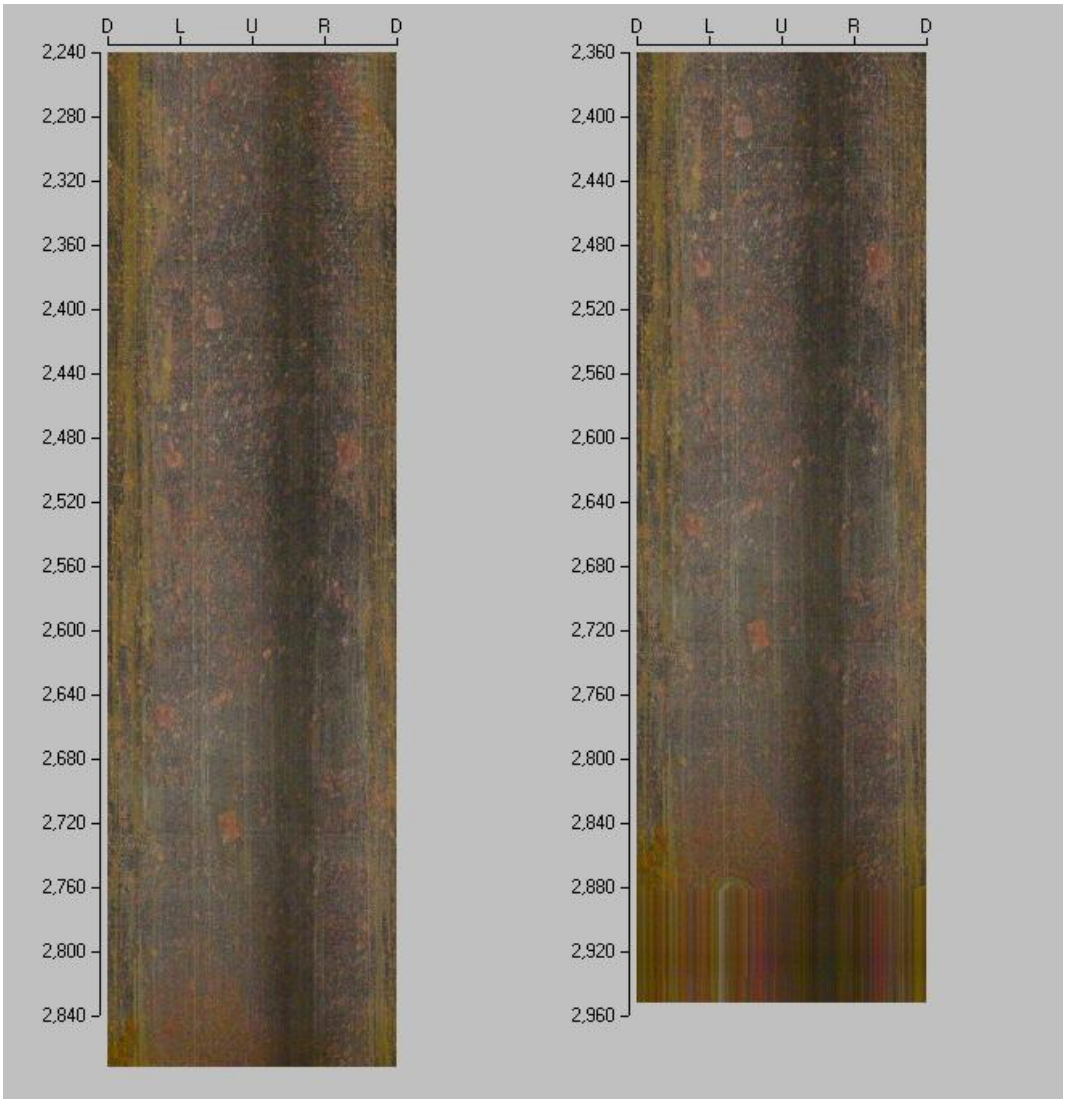
D L U R D
2,240
2,280
2,320
2,360
2,400
2,440
2,480
2,520
2,560
2,600
2,640
2,680
2,720
2,760
2,800
2,840
D L U R D
2,360
2,400
2,440
2,480
2,520
2,560
2,600
2,640
2,680
2,720
2,760
2,800
2,840
2,880
2,920
2,960

A.5. KQ0047B02

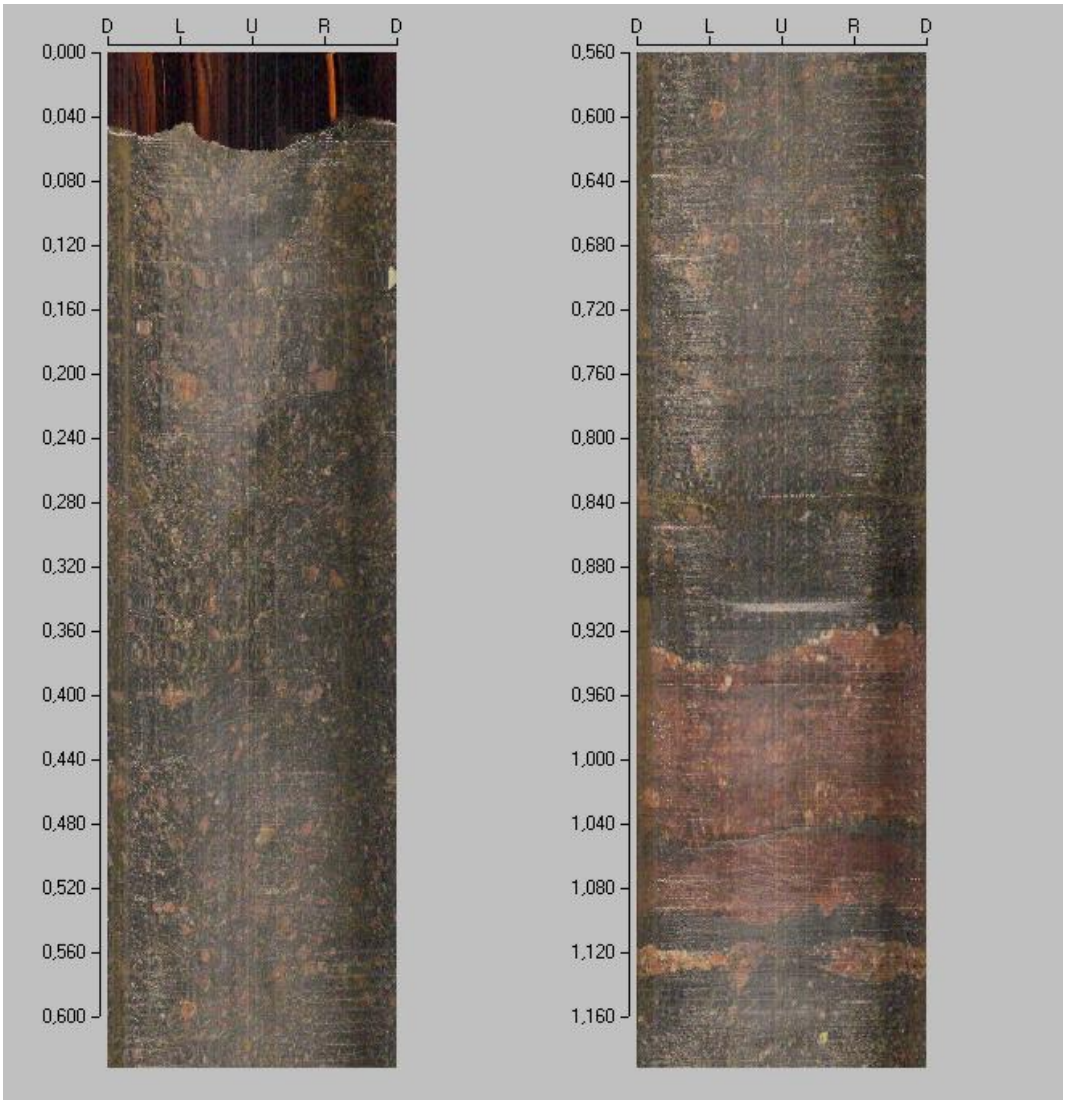

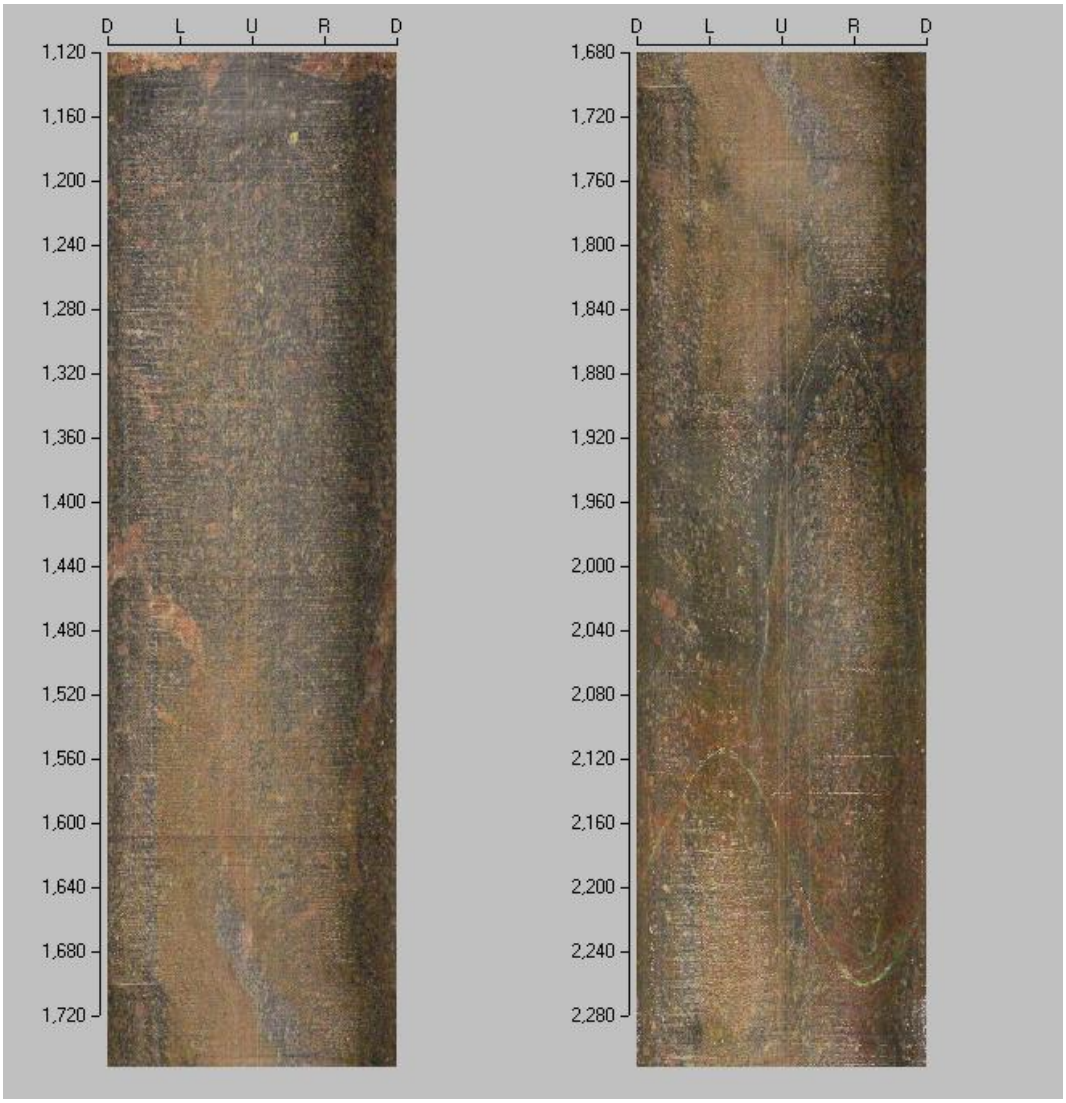
D L U R D
1,120
1,160
1,200
1,240
1,280
1,320
1,360
1,400
1,440
1,480
1,520
1,560
1,600
1,640
1,680
1,720
D L U R D
1,680
1,720
1,760
1,800
1,840
1,880
1,920
1,960
2,000
2,040
2,080
2,120
2,160
2,200
2,240
2,280


D L U R D
2,240
2,280
2,320
2,360
2,400
2,440
2,480
2,520
2,560
2,600
2,640
2,680
2,720
2,760
2,800
2,840
D L U R D
2,360
2,400
2,440
2,480
2,520
2,560
2,600
2,640
2,680
2,720
2,760
2,800
2,840
2,880
2,920
2,960

A.6. KQ0047G01

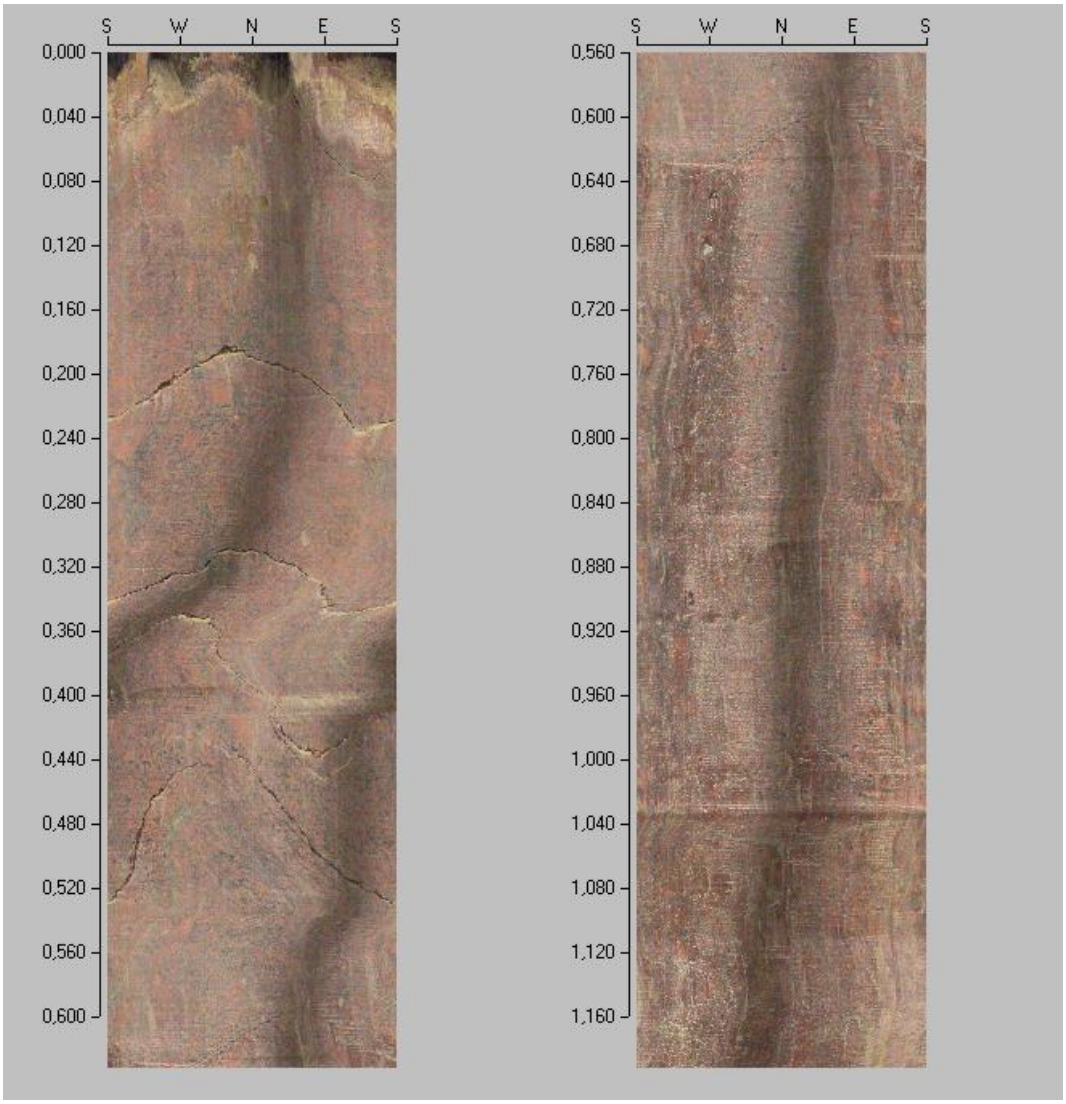

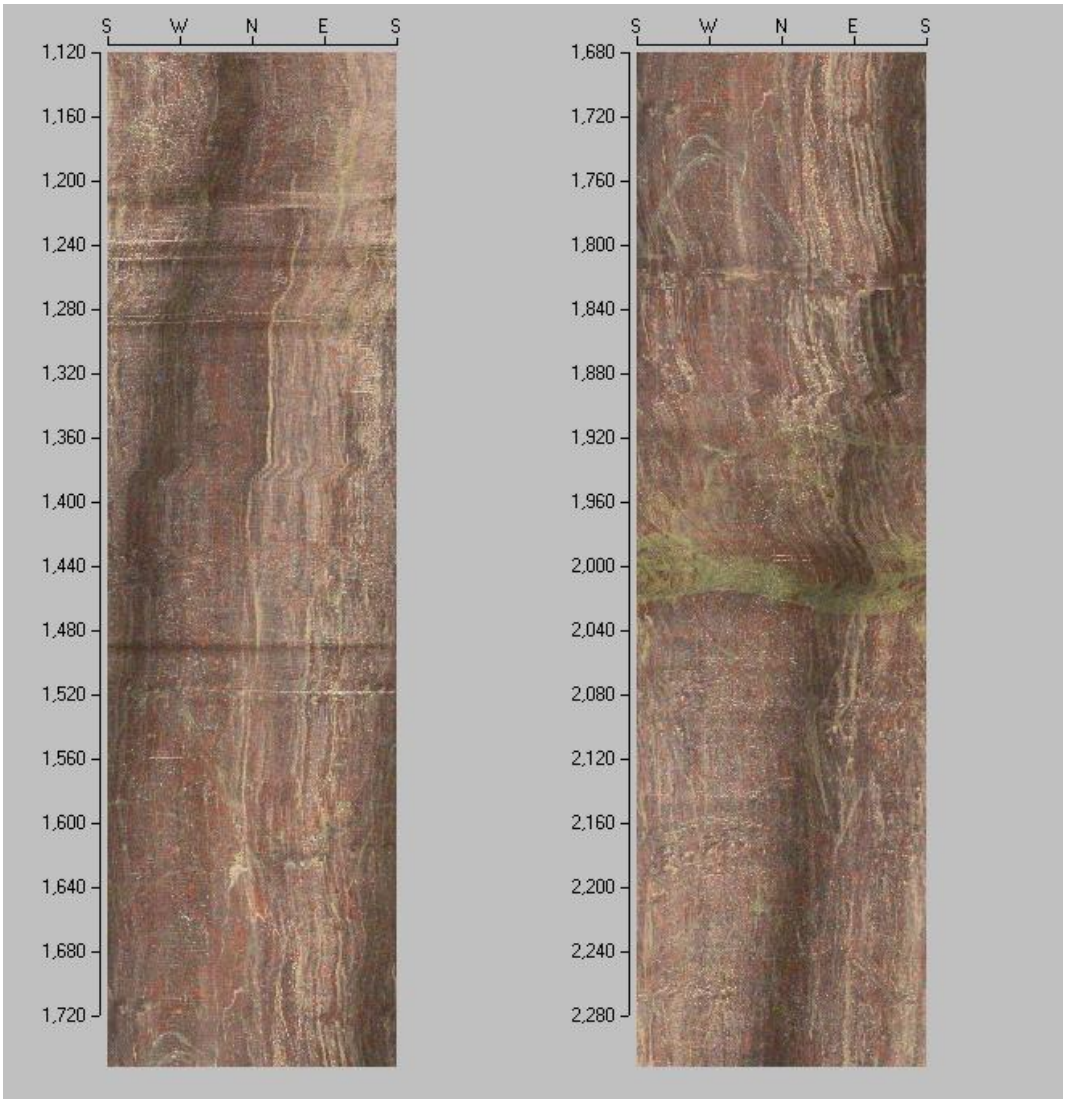
S W N E S
1,120
1,160
1,200
1,240
1,280
1,320
1,360
1,400
1,440
1,480
1,520
1,560
1,600
1,640
1,680
1,720
S W N E S
1,680
1,720
1,760
1,800
1,840
1,880
1,920
1,960
2,000
2,040
2,080
2,120
2,160
2,200
2,240
2,280

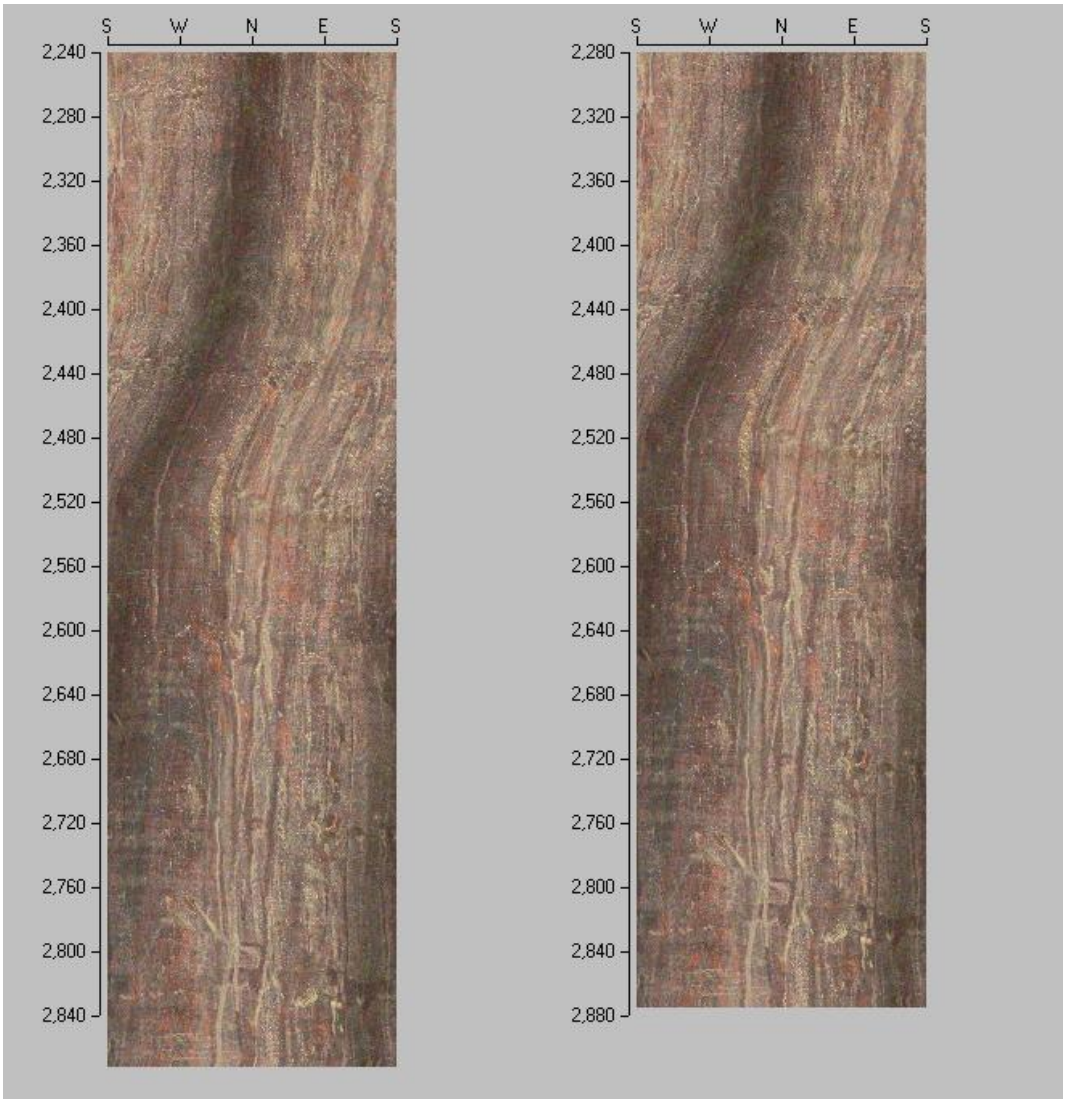
S W N E S
2,240
2,280
2,320
2,360
2,400
2,440
2,480
2,520
2,560
2,600
2,640
2,680
2,720
2,760
2,800
2,840
S W N E S
2,280
2,320
2,360
2,400
2,440
2,480
2,520
2,560
2,600
2,640
2,680
2,720
2,760
2,800
2,840
2,880

A.7. KQ0047H01

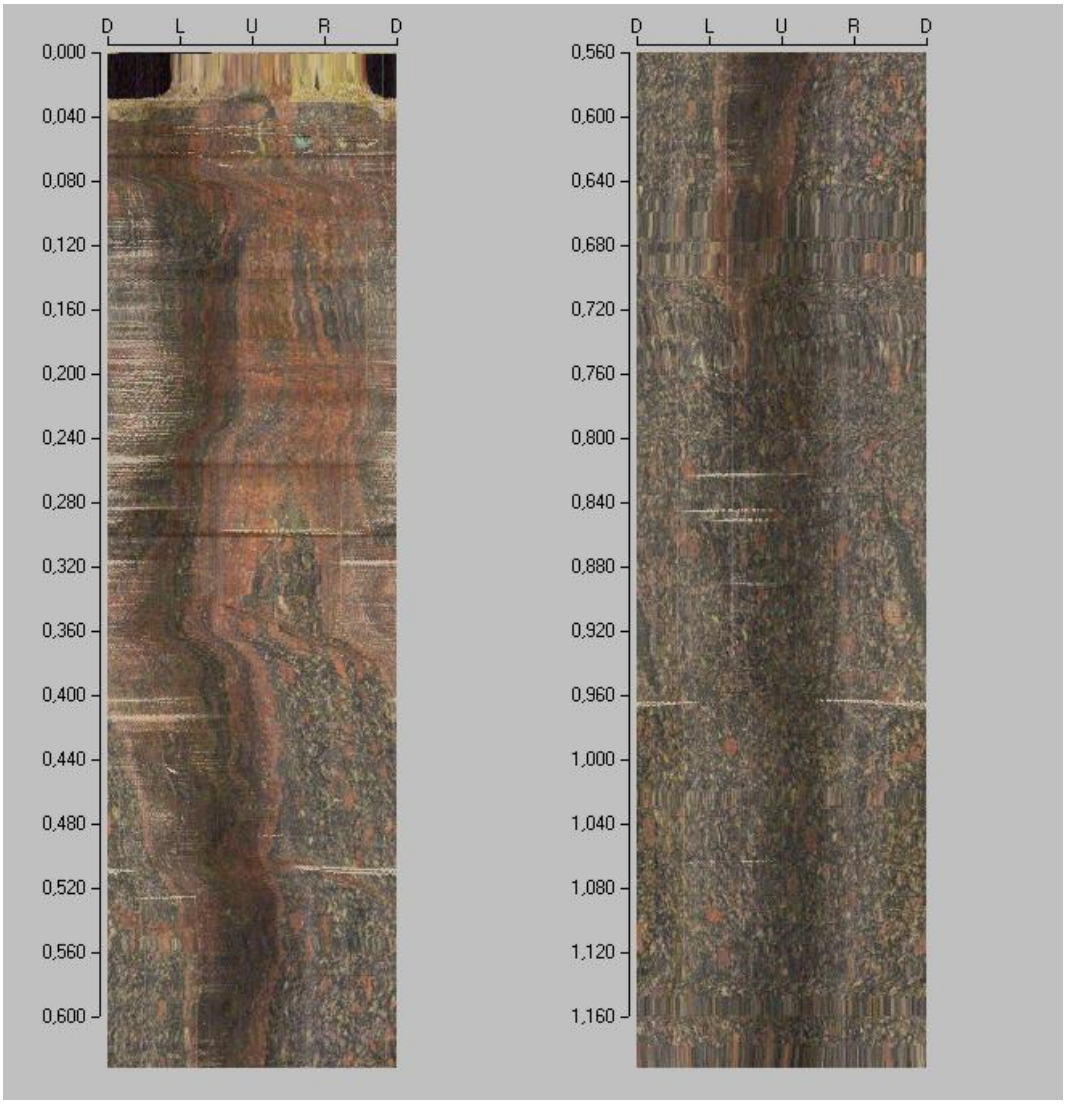

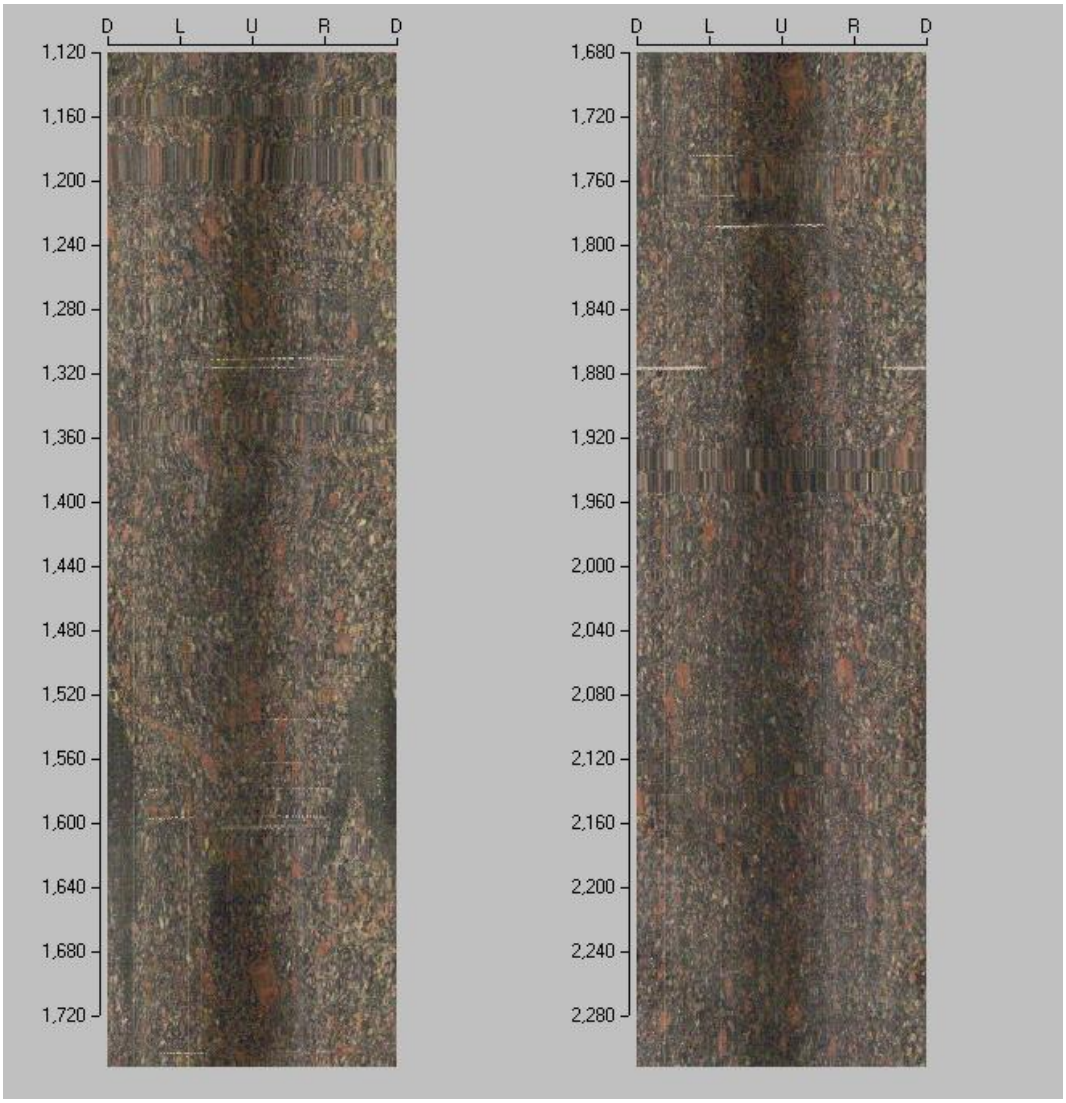
D L U R D
1,120
1,160
1,200
1,240
1,280
1,320
1,360
1,400
1,440
1,480
1,520
1,560
1,600
1,640
1,680
1,720
D L U R D
1,680
1,720
1,760
1,800
1,840
1,880
1,920
1,960
2,000
2,040
2,080
2,120
2,160
2,200
2,240
2,280

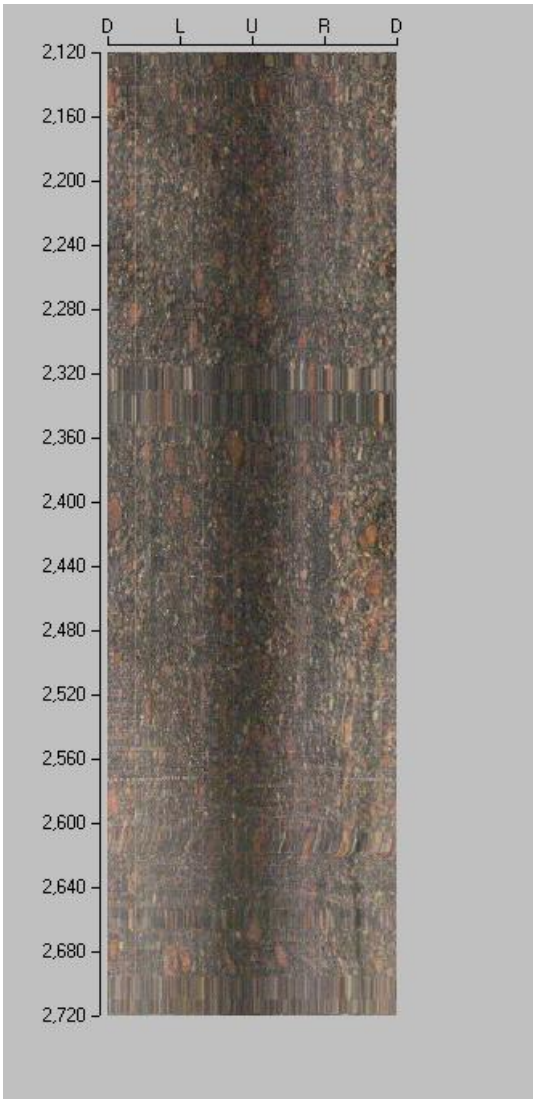
D
L
U
R
D
2,120
2,160
2,200
2,240
2,280
2,320
2,360
2,400
2,440
2,480
2,520
2,560
2,600
2,640
2,680
2,720

A.8. KQ0047I01

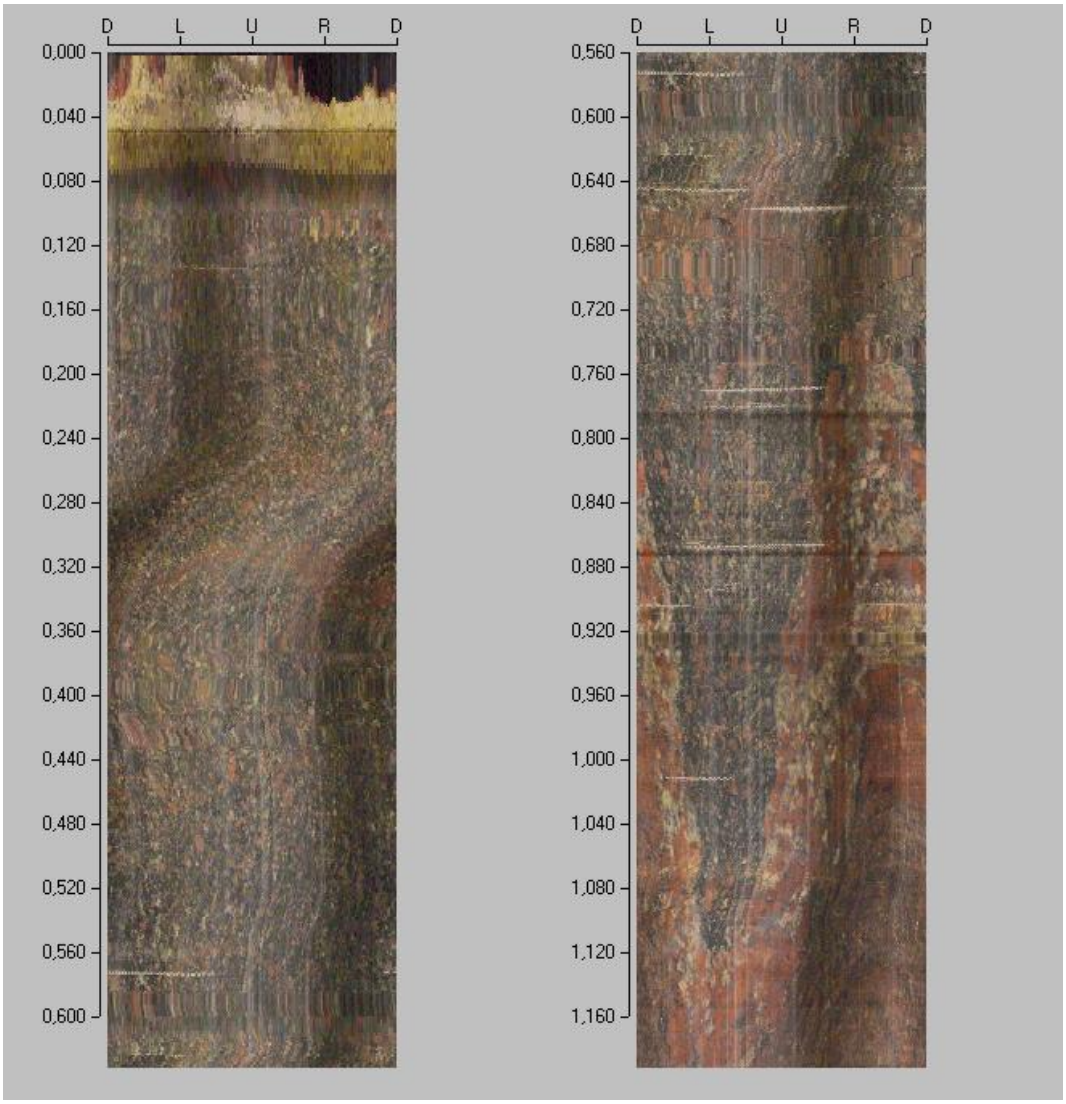


D L U R D
1,120
1,160
1,200
1,240
1,280
1,320
1,360
1,400
1,440
1,480
1,520
1,560
1,600
1,640
1,680
1,720
D L U R D
1,680
1,720
1,760
1,800
1,840
1,880
1,920
1,960
2,000
2,040
2,080
2,120
2,160
2,200
2,240
2,280

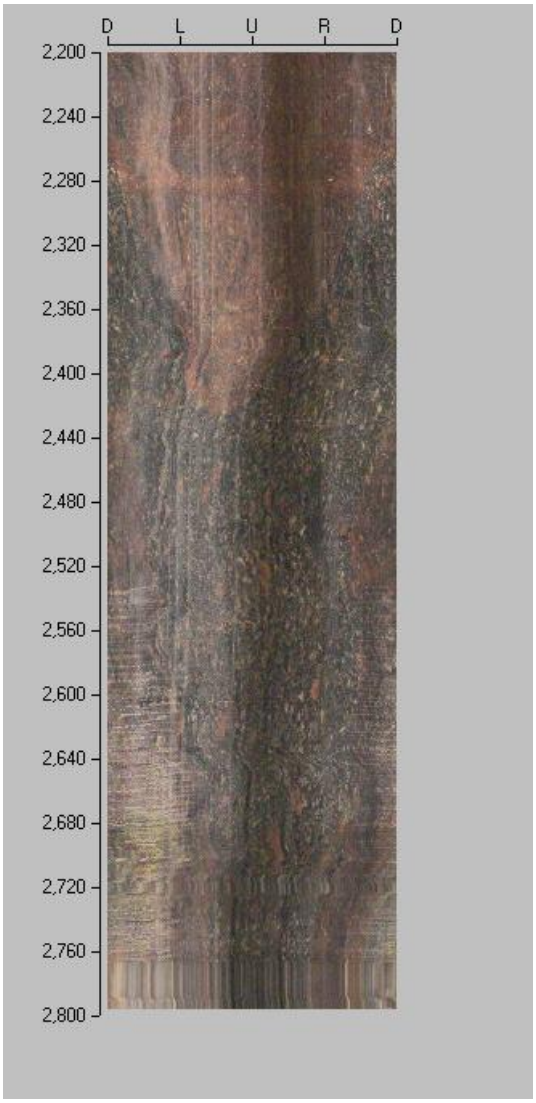
D
L
U
R
D
2,200
2,240
2,280
2,320
2,360
2,400
2,440
2,480
2,520
2,560
2,600
2,640
2,680
2,720
2,760
2,800